



5-1991

Modeling potassium-sulfur interactions across secondary combustor in a coal-fired magnetohydrodynamics (MHD) system

Chun Li

Follow this and additional works at: https://trace.tennessee.edu/utk_gradthes

Recommended Citation

Li, Chun, "Modeling potassium-sulfur interactions across secondary combustor in a coal-fired magnetohydrodynamics (MHD) system. " Master's Thesis, University of Tennessee, 1991.
https://trace.tennessee.edu/utk_gradthes/12455

This Thesis is brought to you for free and open access by the Graduate School at TRACE: Tennessee Research and Creative Exchange. It has been accepted for inclusion in Masters Theses by an authorized administrator of TRACE: Tennessee Research and Creative Exchange. For more information, please contact trace@utk.edu.

To the Graduate Council:

I am submitting herewith a thesis written by Chun Li entitled "Modeling potassium-sulfur interactions across secondary combustor in a coal-fired magnetohydrodynamics (MHD) system." I have examined the final electronic copy of this thesis for form and content and recommend that it be accepted in partial fulfillment of the requirements for the degree of Master of Science, with a major in Chemical Engineering.

Atul C. Sheth, Major Professor

We have read this thesis and recommend its acceptance:

Lloyd W. Crawford, James N. Chapman

Accepted for the Council:

Carolyn R. Hodges

Vice Provost and Dean of the Graduate School

(Original signatures are on file with official student records.)

To the Graduate Council:

I am submitting herewith a thesis written by Jun Li entitled "Modeling Potassium-Sulfur Interactions Across Secondary Combustor in a Coal-Fired Magnetohydrodynamics(MHD) System". I have examined the final copy of this thesis for form and content and recommend that it be accepted in partial fulfillment of the requirements for the degree of Master of Science, with a major in Chemical Engineering.

Atul C. Sheth

Atul C. Sheth, Major Professor

We have read this thesis
and recommend its acceptance:

Lloyd W. Campbell
James W. Chapman

Accepted for the Council :

Lew Minkal

Vice Provost

and Dean of the Graduate School

STATEMENT OF PERMISSION TO USE

In presenting this thesis in partial fulfillment of the requirements for a Master's degree at The University of Tennessee, Knoxville, I agree that the Library shall make it available to borrowers under rules of the Library. Brief quotations from this thesis are allowable without special permission, provided that accurate acknowledgment of the source is made.

Permission for extensive quotation from or reproduction of this thesis may be granted by my major professor, or in his absence, by the Head of Interlibrary Services when, in the opinion of either, the proposed use of the material is for scholarly purposes. Any copying or use of the material in this thesis for financial gain shall not be allowed without my written permission.

Signature _____

John A. ...

Date _____

April 23, 1991

**MODELING POTASSIUM-SULFUR INTERACTIONS
ACROSS SECONDARY COMBUSTOR IN A COAL-FIRED
MAGNETOHYDRODYNAMICS(MHD) SYSTEM**

A Thesis

Presented for the

Master of Science

Degree

The University of Tennessee, Knoxville

Jun Li

May 1991

ACKNOWLEDGMENT

I wish to express my sincere appreciation to my major professor, Dr. Atul C. Sheth, whose knowledge, insight, and care guided me through the study and research in the past two years. I also gratefully acknowledge the invaluable help from Dr. Lloyd W. Crawford, who taught me to apply the computer codes and influenced me by his own hard-working. My sincere appreciation extends to Dr. James N. Chapman, for reading and correcting the manuscript and thereby improving the thesis. I am deeply indebted to Mr. Darryll Rasnake, who helped me so much in preparation of this thesis—collecting the samples, plotting the figures, and deriving the empirical equations.

My sincere thanks are also extended to Mr. Alan Tate, Mr. Phil Sherrill, Mr. Douglas Jackson, Ms. Lisa Blanks, and Mrs. Mary Lo, for their invaluable assistances in sampling, analyzing, providing the mass balance information, drawing the figures, and searching the literature. I also want to thank the Energy Conversion Research & Development Programs(ECP) at the University of Tennessee Space Institute for providing the graduate research assistantship. Finally, I wish to express my sincere appreciation to my wife, Shuying, for her constant support and encouragement in preparing this thesis and in my life.

Wherever errors might remain in this thesis are solely my responsibility. This work was sponsored by the United States Department of Energy under contract No. DE-AC02-79ET10815.

ABSTRACT

The addition of a sulfur-free potassium salt as a seed material is one of the unique characteristics of a coal-fired Magnetohydrodynamics(MHD) power generation system. This potassium seed serves a two-fold purpose— to increase the electrical conductivity of the plasma formed in the primary combustor of an MHD system, and to reduce sulfur-containing pollutant emissions from the flue gas by the formation of spent seed K_2SO_4 . The optimization of performance conditions of an MHD system will eventually depend on how well the interaction of potassium and sulfur in the system is understood. This thesis is focused on modeling the potassium-sulfur interactions in a typical coal-fired MHD power generation system: the Coal-Fired Flow Facility(CFFF) at the University of Tennessee Space Institute(UTSI).

Thermodynamic and kinetic computer codes were used to carry out extensive parametric calculations for the CFFF system. Calculation parameters were chosen based on meaningful operating conditions. Gas and particulate samples from selected locations at the CFFF were collected and analyzed. These results are then compared with those from the calculations. An overall potassium-sulfur interaction model is then postulated. An empirical equation which correlates SO_2 concentration with its major influencing factors is also presented.

According to the model, flame radical/sulfur chemistry and potassium oxidation chemistry are the dominant chemical reactions taking place before the secondary combustion. Potassium-sulfur reaction chemistry becomes dominant after the secondary combustion. From the derived empirical equation, SO_2 concentration is found to depend exponentially on the temperature of secondary combustion gases.

TABLE OF CONTENTS

CHAPTER	PAGE
1. INTRODUCTION	1
1.1 MHD Background	1
1.2 The Coal-Fired Flow Facility at UTSI	2
1.3 Modeling Potassium-Sulfur Interactions – Major Objective	4
1.4 Approach	6
2. COMPUTER CODE MODIFICATION AND PARAMETER DETERMINATION	8
2.1 NASA SP-273 Equilibrium Code	8
2.2 Modifications to NASA SP-273 Computer Code	11
2.3 COAL Program and Its Modification	12
2.4 Parameter Determination	15
3. CALCULATED RESULTS AND INTERPRETATIONS	23
3.1 Potassium and Sulfur Species at Equilibrium	23
3.2 SO ₂ and H ₂ S Behavior before Secondary Combustion	27
3.2.1 SO ₂ and H ₂ S Behavior with respect to Gas Temperature	27
3.2.2 SO ₂ and H ₂ S Behavior with respect to K ₂ /S Ratio	29
3.2.3 SO ₂ and H ₂ S Behavior with respect to Primary Stoichiometric Ratio	29
3.3 SO ₂ Behavior after Secondary Combustion	31

3.3.1	SO ₂ Behavior with respect to Secondary Stoichiometric Ratio	31
3.3.2	SO ₂ Concentration with respect to K ₂ /S Ratio	33
3.4	Potassium Species Behavior before and after Secondary Combustion	36
3.4.1	The Effect of SR1 on K, KOH before Secondary Combustion	38
3.4.2	The Effect of K ₂ /S Ratio on K, KOH before Secondary Combustion	40
3.4.3	The Effect of K ₂ /S on KOH, K ₂ SO ₄ (c) after Secondary Combustion	42
3.4.4	The Effect of SR2 on KOH and K ₂ SO ₄ (c) after Secondary Combustion	44
3.5	Behavior of Minor Sulfur Species	44
3.6	The Concentration of Gas Phase KS, K ₂ S, K ₂ SO ₄ Species	48
4.	COAL-FIRED FLOW FACILITY MEASUREMENTS	51
4.1	Sampling System	51
4.2	Sampling Process	57
4.3	Data Analysis for Particulate and Gaseous Species	58
5.	COMPARISON OF RESULTS AND PROPOSED POTASSIUM-SULFUR REACTION STOICHIOMETRY	62
5.1	Comparison of Calculated Results with CFFF Measurements	62
5.2	PROF Code Modeling	67
5.3	Proposed Potassium-Sulfur Reaction Stoichiometry	70
5.3.1	Release of Coal-Bound Sulfur	70
5.3.2	The Formation of Reduced Form of Sulfur Species	71

5.3.3 Decomposition of Seed and Oxidation of Potassium	72
5.3.4 Dominant Chemistry before Secondary Combustion	73
5.3.5 Potassium-Sulfur Reaction Chemistry after Secondary Combustion	73
5.3.6 Overall Potassium-Sulfur Reaction Model	75
5.4 Empirical Equations for SO ₂ Concentration after Secondary Combustion	78
5.4.1 Parameters Influencing SO ₂ Concentration	78
5.4.2 An Empirical Equation for SO ₂ Concentration	80
5.4.3 Sensitivity Analysis	84
5.5 Error Sources	87
6. CONCLUSIONS AND RECOMMENDATIONS	89
6.1 Conclusions	89
6.2 Recommendations	90
LIST OF REFERENCES	92
APPENDICES	96
APPENDIX A. CALCULATION OF POTASSIUM LOSS AS K ₂ O IN THE RADIANT FURNACE SLAG	97
APPENDIX B. H ₂ S MEASUREMENTS IN THE CFFF FOR EARLY TESTS	99
APPENDIX C. THE INPUT FILE FOR PROF MODELING	100
VITA	103

LIST OF TABLES

TABLE	PAGE
I. Typical Operating Conditions at Primary Combustor	15
II. Typical Operating Conditions at Secondary Combustor	16
III. Coal and Ash Analysis for Test LMF4-R	17
IV. Fuel Oil Analysis for Test LMF4-R	17
V. Slag Analysis for Recent LMF4 Tests	21
VI. Slag Removal at Radiant Furnace	21
VII. Molar Fraction of Potassium Species before Secondary Combustion($K_2/S=1.25$, $SR1=0.85$)	24
VIII. Molar Fraction of Potassium Species after Secondary Combustion($K_2/S=1.25$, $SR1=0.85$, $SR2=1.10$)	24
IX. Molar Fraction of Sulfur Species before Secondary Combustion($K_2/S=1.25$, $SR1=0.85$)	25
X. Molar Fraction of Sulfur Species after Secondary Combustion($K_2/S=1.25$, $SR1=0.85$, $SR2=1.10$)	25
XI. Particulate Analysis for Test LMF4-U	59
XII. SO_2 Measurements for Test LMF4-U	60

XIII. H ₂ S Measurements for Test LMF4-U	60
XIV. Coal and Ash Analysis for Test LMF4-U	63
XV. Fuel Oil Analysis for Test LMF4-U	63
XVI. Major Operating Conditions for Test LMF4-U	64
XVII. Concentrations of Major Gas Phase Sulfur Species for Test LMF4-U	65
XVIII. Concentrations of Condensed Phase Species for Test LMF4-U	65
XIX. Results from PROF Calculation for Test LMF4-U at the RF1 Sampling Probe	69
XX. Sensitivity of SO ₂ Concentration to Gas Temperature at SR2=1.10	84
XXI. The Effects of Operating Parameters on Major Species	90

LIST OF FIGURES

FIGURE	PAGE
1- 1. Coal-Fired Low-Mass Flow Facility at UTSI	3
1- 2. Overview of Potassium-Sulfur Interactions in the CFFF	5
3- 1. Fraction of Total Sulfur Species as SO ₂ or H ₂ S vs. Temperature (K ₂ /S=1.25, SR1=0.85)	28
3- 2. Fraction of Total Sulfur Species as SO ₂ or H ₂ S vs. Temperature at Different K ₂ /S Ratios (SR1=0.85)	30
3- 3. Fraction of Total Sulfur Species as SO ₂ vs. Temperature at Different SR1 (K ₂ /S=1.00)	30
3- 4. Fraction of Total Sulfur Species as H ₂ S vs. Temperature at Different SR1 (K ₂ /S=1.00)	32
3- 5. Fraction of Total Sulfur Species as SO ₂ vs. Temperature at Different SR2 (K ₂ /S=1.00, SR1=0.85)	32
3- 6. Fraction of Total Sulfur Species as SO ₂ vs. Temperature at Different SR2 (K ₂ /S=1.25, SR1=0.85)	34
3- 7. SO ₂ Concentrations (wet basis) vs. Temperature at Different K ₂ /S Ratios (SR2=1.05)	34

3- 8. Fraction of Total Potassium Species as Major Potassium Species vs. Temperature before Secondary Combustion ($K_2/S=1.25$, $SR1=0.85$)	37
3- 9. Fraction of Total Potassium Species as Major Potassium Species vs. Temperature after Secondary Combustion ($K_2/S=1.25$, $SR1=0.85$, $SR2=1.05$)	37
3-10. Fraction of Total Potassium Species as Gas Phase K vs. Temperature at Different $SR1$ ($K_2/S=1.25$)	39
3-11. Fraction of Total Potassium Species as Gas Phase KOH vs. Temperature at Different $SR1$ ($K_2/S=1.25$)	39
3-12. Fraction of Total Potassium Species as Gas Phase K vs. Temperature at Different K_2/S Ratios ($SR1=0.85$)	41
3-13. Fraction of Total Potassium Species as Gas Phase KOH vs. Temperature at Different K_2/S Ratios ($SR1=0.85$)	41
3-14. Fraction of Total Potassium Species as Condensed $K_2SO_4(c)$ vs. Temperature at Different K_2/S Ratios ($SR1=0.85$, $SR2=1.05$) . . .	43
3-15. Fraction of Total Potassium Species as Gas Phase KOH vs. Temperature at Different K_2/S Ratios ($SR1=0.85$, $SR2=1.05$) . . .	43
3-16. Fraction of Total Potassium Species as Condensed $K_2SO_4(c)$ vs. Temperature at Different $SR2$ ($K_2/S=1.25$, $SR1=0.85$)	45

3-17. Fraction of Total Potassium Species as Gas Phase KOH vs. Temperature at Different SR2 ($K_2/S=1.25$, $SR1=0.85$)	45
3-18. Fraction of Total Sulfur Species as Minor Sulfur Species vs. Temperature before Secondary Combustion ($K_2/S=1.25$, $SR1=0.85$)	46
3-19. Fraction of Total Sulfur Species as COS vs. Temperature at Different SR1 ($K_2/S=1.25$)	46
3-20. Fraction of Total Sulfur Species as SO vs. Temperature at Different SR1 ($K_2/S=1.25$)	47
3-21. Fraction of Total Sulfur Species as S_2 vs. Temperature at Different SR1 ($K_2/S=1.25$)	47
3-22. Fraction of Total Sulfur Species as Gas Phase K_2S vs. Temperature at Different K_2/S Ratios ($SR1=0.85$)	49
3-23. Fraction of Total Sulfur Species as Gas Phase K_2SO_4 vs. Temperature at Different K_2/S Ratios ($SR1=0.85$, $SR2=1.05$)	49
4- 1. Sampling Locations in the CFFF	52
4- 2. Aspirated Particulate and Gas Sampling System	53
4- 3. Sampling Probe	55
4- 4. Sampling Box	56
4- 5. SO_2 Emissions at the Stack from CFFF	61

5- 1. Overall Potassium-Sulfur Interactions Model at the CFFF	76
5- 2. SO ₂ Concentrations (wet basis) after Secondary Combustion vs. Temperature at Different SR1 (K ₂ /S=1.25, SR2=1.05)	79
5- 3. SO ₂ Concentrations (wet basis) after Secondary Combustion vs. Temperature at Different K ₂ /S Ratios (SR1=0.85, SR2=1.10)	81
5- 4. SO ₂ Concentrations (wet basis) after Secondary Combustion vs. Temperature at Different SR2 (K ₂ /S=1.25, SR1=0.85)	81
5- 5. SO ₂ Concentration (wet basis) after Secondary Combustion vs. K ₂ /S Ratio at Different Temperatures (SR1=0.85, SR2=1.05)	82
5- 6. SO ₂ Concentration (wet basis) after Secondary Combustion vs. SR2 at Different Temperatures (K ₂ /S=1.25, SR1=0.85)	82
5- 7. Comparison of Model Predictions with Equilibrium Calculations	85
5- 8. Comparison of Model Predictions with CFFF Measurements	85
5- 9. Sensitivity of SO ₂ Concentration with respect to K ₂ /S Ratio (SR1=0.85, SR2=1.10)	86
5-10. Sensitivity of SO ₂ Concentration with respect to SR2 (K ₂ /S=1.25, SR1=0.85)	86

LIST OF SYMBOLS

A	cross sectional area
$a_{i,j}$	number of kilogram-atoms of element i per kilogram-mole of species j
b_i	number of kilogram-atoms of element i per kilogram of mixture
b_i^0	number of kilogram-atoms of element i per kilogram of total reactants
C_w	circumference of bounding tube
g	mass specific Gibbs free energy
ΔG^0	standard molar Gibbs function for a chemical reaction
h	enthalpy of bulk gas
$J_{w,i}$	flux of species i at bounding tube wall
K_2/S	potassium-to-sulfur molar ratio
K_p	equilibrium constant
l	number of elements
\dot{m}	mass rate of gas
n	number of kilogram-moles per kilogram of mixture
N	number of species
N_g	number of gas species
n_j	number of kilogram-moles of species j per kilogram of mixture
P	pressure
Q	volumetric heat loss
q_w	heat transport at the bounding tube wall
R	gas constant
ROC	ratio of flow rate (wt) for oil-to-coal
s	distance along flow axis
T	temperature

- V specific volume
 W_i chemical production rate of species i
 Y_i mass fraction of species i

Greek Letters

- γ potassium-to-sulfur ratio (K₂/S)
 μ_j chemical potential per kilogram-mole of species j
 μ_j^0 chemical potential per kilogram-mole of species j in the standard state
 λ_i Lagrangian multiplier for i th constraint
 θ secondary stoichiometric ratio (SR2)

Abbreviation

- BH* Baghouse
CFFF Coal-Fired Flow Facility
ESP Electrostatic Precipitator
LMF Low-Mass Flow
RF1 Radiant Furnace Probe 1
SCI Secondary Combustor Inlet
SCO Secondary Combustor Outlet
SR Stoichiometric Ratio
SR1 Primary Stoichiometric Ratio
SR2 Secondary Stoichiometric Ratio

CHAPTER 1

INTRODUCTION

1.1 MHD Background

Magnetohydrodynamics, MHD, power generation system involves the conversion of kinetic or potential (pressure-volume) energy of a fluid into electrical power by interaction of the fluid with a magnetic field. For this interaction to occur, the fluid must be moving and it must also be an electrical conductor, according to Faraday's law.

The fluid is a high-temperature (up to 3030 K), high pressure (about 8 atm) combustion product from coal mixed with oxygen-enriched air in a coal-fired MHD power generation system. The derived fluid expands through a nozzle to reach a high velocity (subsonic to supersonic), and then passes through a magnetic field region. To increase the electrical conductivity of the fluid gases, an easily ionizable substance, such as potassium in the form of K_2CO_3 , is added to coal before it enters the combustor. This substance is called seed.

It is the addition of seed that makes an MHD power generation system potentially superior to conventional ones. First, seeded gas has the required electrical conductivity. It passes through a magnetic field, converting its kinetic energy directly into electrical energy. Thus the overall efficiency of an MHD power plants could be increased up to 50-55%. Second, seed species will react with fuel-bound sulfur through the process, reducing the sulfur bearing pollutant emissions to almost zero.

This second advantage of an MHD power generation system has been demonstrated at the University of Tennessee Space Institute (UTSI). UTSI is cur-

rently under a contract with the U.S. Department of Energy(DOE) to provide testing and evaluation in a 28 MWt low-mass-flow(LMF) facility, usually known as Coal-Fired Flow Facility(CFFF).

1.2 The Coal-Fired Flow Facility at UTSI

DOE's Coal-Fired Flow Facility, located at UTSI, consists of upstream and downstream components. Figure 1-1 shows the CFFF. The upstream includes vitiation heater, primary combustor, nozzle, aerodynamic channel, and diffuser. The downstream includes radiant furnace, secondary combustor, superheater, air heater, electrostatic precipitator(ESP), baghouse, venturi scrubber/cyclone system, and stack. At UTSI, efforts are focused on testing and evaluation of the downstream components. A dummy duct along the channel is used in place of the MHD generator to simulate time-temperature history.

During the test, fuel oil is first burnt with oxygen-enriched air in vitiation heater to raise the temperature of the oxidizer. Then vitiated oxidizer is mixed with the mixture of K_2CO_3 seed and pulverized coal at fuel-rich condition in the primary combustor, where it is combusted at high temperature and high pressure to create a plasma. The resulting plasma expands through a nozzle to obtain a high velocity. As the plasma passes through the channel section, electricity would be induced if the MHD generator were installed. The kinetic energy could be thus converted into electrical energy. Its velocity is then reduced by expanding through the diffuser.

Radiant furnace, offering enough residence time, cools the combustion gases and thereby allows the NO_x formed at the upstream to decompose. It also rejects a major part of the slag. Partially combusted gases then flow into secondary combustor, where the combustion is completed with addition of excess

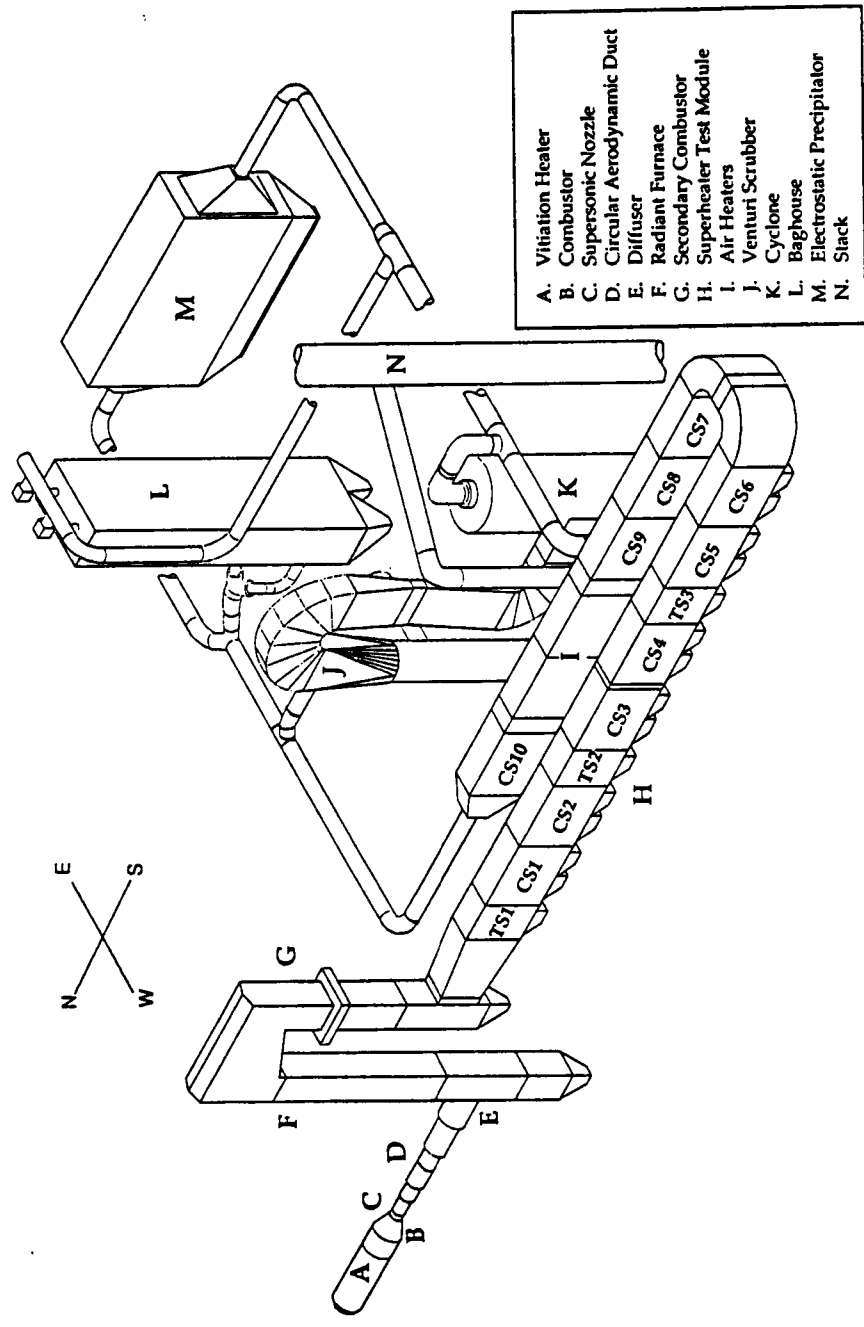


Figure 1-1. Coal-Fired Low-Mass Flow Facility at UTSI

secondary air. The combustion products then continuously pass through heat recovery devices (superheater, air heater), and particulate control devices (BH, ESP), and finally exit from the stack.

As described above, the working fluid in an MHD process is a chemically reacting flow. It also differs from the reacting flow in conventional combustion processes because of the high reactivity and concentration of potassium seed. Consequently, some research efforts are emphasized to investigate the interactions of potassium with other materials, such as sulfur, slag, etc. This thesis is concentrated mainly on investigating the potential interactions between potassium and sulfur species.

1.3 Modeling Potassium-Sulfur Interactions—Major Objective

Figure 1-2 shows the outline of overall potassium-sulfur chemistry at CFFF. Seed is added in the form of K_2CO_3 . As combustion products flow down through the system, part of the potassium is tied up with oxide of aluminum and silicon as insoluble aluminosilicates ($KAlSiO_4$), majority of which is then rejected in the radiant furnace as slag. The major part of the potassium reacts with coal-bound sulfur, and is collected as spent seed in the form of K_2SO_4 . Most of the spent seed (above 95%) should be recovered, and regenerated as potassium carbonate or potassium formate with usable or disposable sulfur compounds as its end/waste products. Regenerated K_2CO_3 is recycled as seed to the primary combustor. A minor part of sulfur left in the gas phase exits from the system, following emission guidelines.

The best schemes of minimizing SO_2 emission, minimizing potassium losses through slag, and maximizing the spent seed recovery are still under development. In addition, the effects of potassium-sulfur chemistry on plasma

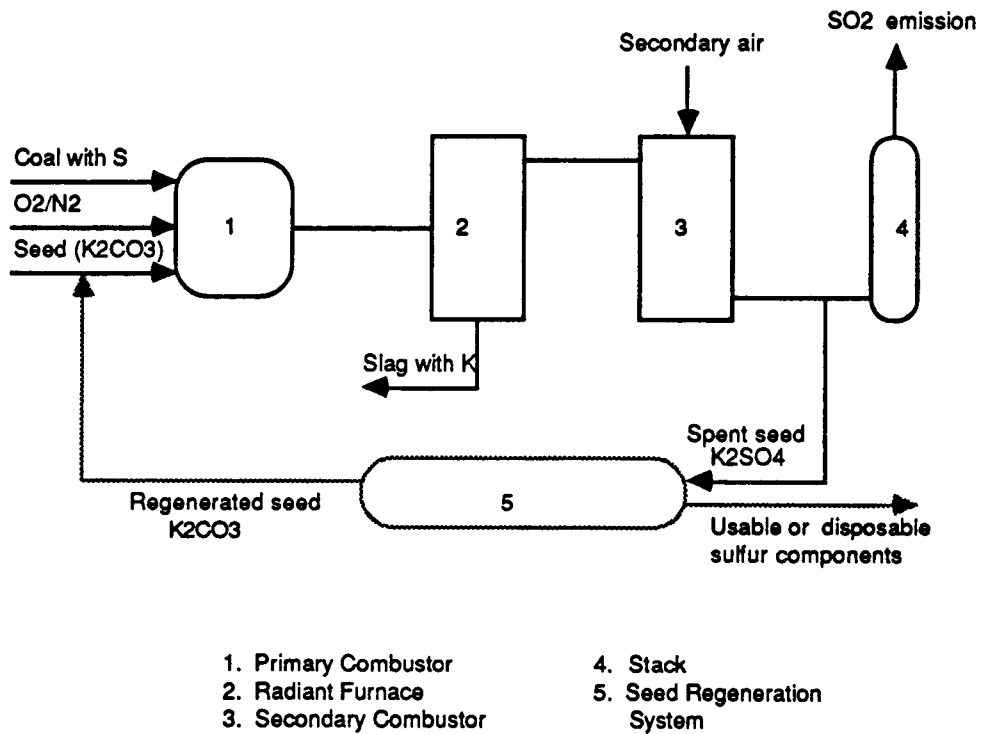


Figure 1-2. Overview of Potassium-Sulfur Interactions in the CFFF

conductivity, equipment corrosion, etc., are not very clear. From the standpoint of chemical engineering, the more we know about the reacting materials and how they react, the more assurance we will have for proper design.

Very few literature articles have been published discussing the potassium and sulfur interactions in a coal-fired MHD system. In the few published ones [1,2], the model that predicts the reaction between potassium and sulfur is incomplete/insufficient due to lack of proper thermodynamic data or unrealistic assumptions. Therefore, it is necessary to establish a model of potassium-sulfur interactions that truly reflects the real coal-fired MHD system.

The primary objective of the present work is then to set up a model that could predict compositions and concentrations of various potassium and sulfur species in a coal-fired MHD system under different operating conditions.

The second objective is to investigate or hypothesize the possible chemical reactions, homogeneously or heterogeneously, taking place at different locations in the CFFF.

1.4 Approach

There are three areas of investigation for a chemical reaction, the overall stoichiometry, the kinetics, and the mechanism. Since the overall stoichiometry of potassium-sulfur reaction has not been fully characterized, the proposed work is focused on the study of stoichiometry of potassium-sulfur reactions.

The approach involves a significant amount of numerical calculations, experimental measurements and analyses, and theoretical analyses. Thermodynamic [3] and kinetic [4] computer codes are used and modified to calculate properties of various species in the CFFF system. Gas and condensed phase samples are collected from the CFFF system across the secondary combustor area, where

the temperature range (1800 - 1100 K) and system environment (from reducing to oxidizing) are particularly suited for potassium-sulfur reactions. The calculated results are then compared with the measured ones. Based on these results, the effects of operating conditions on the behavior of major potassium and sulfur species are investigated. Overall potassium-sulfur reaction stoichiometries are also investigated. In addition, an empirical equation, which correlates the SO_2 concentration to gas temperature, potassium-to-sulfur(K_2/S) molar ratio, and secondary stoichiometric ratio(SR_2 , defined in the following chapter), is derived. A preliminary potassium-sulfur interaction model is thus established.

CHAPTER 2

COMPUTER CODE MODIFICATION AND PARAMETER DETERMINATION

2.1 NASA SP-273 Equilibrium Code

Multicomponent equilibrium state is the limit of a chemically reacting flow. By knowing the properties of a complex reacting system at equilibrium, one could know the ultimate degree of reactions of the system. Three schemes for determination of equilibrium states at specified temperature and pressure may be considered, namely Gibbs free energy minimization, equilibrium constant formulation, and equating of forward and reverse reaction rates. A vastly superior computational scheme is the Gibbs free energy minimization approach, which has been formulated by Gordon and McBride [3].

For a mixture of reacting gases at prescribed temperature and pressure, chemical equilibrium is obtained when the Gibbs free energy of the mixture is at minimum, subject to conservation of atomic species as specified in the set of initial reactant mole numbers.

The mass specific Gibbs free energy for a mixture of N species is given by

$$g = \sum_{j=1}^N n_j \mu_j \quad (2.1)$$

where n_j is the number of kilogram-moles of species j per kilogram of mixture, μ_j is the chemical potential per kilogram mole of species j . The mass balance constraints of l elements are:

$$\sum_{j=1}^N a_{ij}n_j - b_i^0 = 0 \quad i = 1, \dots, l \quad (2.2)$$

or

$$b_i - b_i^0 = 0 \quad i = 1, \dots, l \quad (2.3)$$

where the coefficient $a_{i,j}$ is the number of kilogram-atoms of element i per kilogram-mole of species j , b_i^0 is the assigned number of kilogram-atoms of element i per kilogram of total reactants (fuel and oxidant), and

$$b_i = \sum_{j=1}^N a_{i,j}n_j \quad i = 1, \dots, l \quad (2.4)$$

is the number of kilogram-atoms of element i per kilogram of mixture.

Following the Lagrangian method, we define

$$G = g + \sum_{i=1}^l \lambda_i (b_i - b_i^0) \quad (2.5)$$

where λ_i is the Lagrangian multiplier that incorporates the i th constraint in equation (2.3). The necessary condition for equilibrium then becomes

$$\begin{aligned} \delta G &= \delta g + \sum_{i=1}^l \lambda_i \delta (b_i - b_i^0) + \sum_{i=1}^l (b_i - b_i^0) \delta \lambda_i \\ &= \sum_{j=1}^N \mu_j \delta n_j + \sum_{i=1}^l \lambda_i \sum_{j=1}^N a_{i,j} \delta n_j + \sum_{i=1}^l (b_i - b_i^0) \delta \lambda_i \\ &= \sum_{j=1}^N (\mu_j + \sum_{i=1}^l \lambda_i a_{i,j}) \delta n_j + \sum_{i=1}^l (b_i - b_i^0) \delta \lambda_i \\ &= 0 \end{aligned} \quad (2.6)$$

Treating the variations δn_j and $\delta \lambda_i$ as independent gives

$$\mu_j + \sum_{i=1}^l \lambda_i a_{i,j} = 0 \quad j = 1, \dots, N \quad (2.7)$$

and

$$b_i - b_i^0 = 0 \quad i = 1, \dots, l \quad (2.3)$$

It is assumed that all gases are ideal and interactions among phases may be neglected. The equation of state can be applied to the mixture:

$$PV = nRT \quad (2.8)$$

where P is pressure(N/m²), V specific volume(m³/kg), n moles(kg-mole/kg), T temperature(K), and R gas constant($R=8314.3$ J/(kg-mole)(K)). This equation is assumed to be correct even when small amounts of condensed species (up to several percent by weight) are present.

For an ideal gas the chemical potential can be written as

$$\mu_j = \mu_j^0 + RT \ln(n_j/n) + RT \ln(P/P^0) \quad j = 1, \dots, N_g \quad (2.9)$$

where N_g is the number of gas species.

For condensed species

$$\mu_j = \mu_j^0 \quad j = N_g + 1, \dots, N \quad (2.10)$$

where μ_j^0 is the chemical potential in the standard state.

Equations (2.3), (2.7), (2.9), (2.10) required to obtain equilibrium composition are not all linear. Iteration procedures must be used in order to solve these equations. In this code, the steepest descent Newton-Raphson method is applied, obtaining molar fractions of species at equilibrium

$$x_j = \frac{n_j}{n} \quad (2.11)$$

as solutions and output.

2.2 Modifications To NASA SP-273 Computer Code

Modifications to NASA SP-273(NASA code) equilibrium code are simply addition of several new output options. The code originally has one output form: molar fractions of species over total moles of gas and condensed phase species. New added output options include: weight fractions of condensed species over total weight of condensed phase species, dry molar fractions of gas species over total moles of gas phase species, molar percentages of potassium species over total potassium species, molar percentages of sulfur species over total sulfur species, molar ratios of total potassium species in the gas phase over that in the condensed phase, and molar ratios of total sulfur species in the gas phase over that in the condensed phase.

With these new output options, it becomes easier to compare calculated and measured results. As is probably known, gas phase and condensed phase samples are taken and analyzed separately. Readings from gas analysis instrument are usually volume fractions(molar fractions) over total gas species. Some of the instruments require dry gas samples. The analytical results of condensed phase species are reported as weight fractions. These results cannot be compared directly with the original output of NASA code. With these new output options, it is also easier to investigate the behavior of potassium and sulfur species at equilibrium. The distribution of potassium and sulfur species as a whole and in different phases are reflected in these outputs.

To add these options, Subroutines SEARCH, EQLBRM, and OUT of the NASA code need to be modified. In Subroutine SEARCH, commands of calculating molecular weight of possible species are added. In Subroutine EQLBRM, total moles of gas species are first calculated. Moisture moles are then subtracted from these total moles, giving the total moles of gas species on a dry basis. Moles of a gas species divided by the total moles of gas species on the dry basis gives the dry molar fractions of the gas species. Also in this Subroutine, weights of condensed species and their total weight are calculated, giving the weight fractions of condensed species. In Subroutine OUT, possible potassium and sulfur species are searched first. Total moles of potassium species and sulfur species are then calculated. Dividing moles of a potassium species by total moles of potassium species gives the molar percentage of the potassium species in a particular form. Similarly, molar percentages of sulfur species are calculated. Again in this Subroutine, total moles of potassium species in the gas phase, that in the condensed phase, and their respective ratios are calculated. The molar ratios of total sulfur species in gas phase and in condensed phase are calculated similarly.

2.3 COAL Program and Its Modification

When applying the NASA code to coal combustion processes, one has to perform a lot of calculations to set up the input data for the program, because chemical composition varies for different types of coal and operating conditions need extensive adjusting. A natural choice is to write a computer program to do all these calculations.

At UTSI, a FORTRAN program named COAL [5] has been written. This

program is able to set up the input data in the required format and to facilitate certain options, such as moisture level in the fired coal, type of seed, amount of seed, composition of the oxidant, preheat levels, stoichiometry, combustor pressure, magnet size, Mach number at channel entrance, an estimate of the MHD/steam power plant size and others. Additionally, this program: (1). computes the amount of seed required to provide the desired potassium levels specified by the user in percent of the total flow, (2). computes a heat loss for the combustor in calories per gram of total mass flow, and (3). determines the potassium-to-sulfur (K_2/S) ratio.

A significant modification has been made on the COAL program, making it more closely adapt to the CFFF operating situation. The modified COAL program is referred to as M-COAL in the following descriptions.

(1). Fuel oil data are included by M-COAL. In the CFFF at UTSI, fuel oil is used as fuel other than coal to simulate coal combustion process with certain percent slag rejection (or certain percent coal ash carry over) before the plasma passes through the channel. Therefore, it is necessary to include the fuel oil information when modeling the CFFF combustion process. The M-COAL reads in: (1) fuel oil analysis based on ASTM standard; and (2) fuel oil-to-coal ratio (by mass flow rate). It then normalizes the fuel oil analysis data, and writes the fuel oil data in proper form as required by NASA code.

(2). K_2/S ratio is chosen as another option to specify the amount of seed. K_2/S ratio is an intuitive parameter. It reflects the stoichiometric amount of seed needed to convert all the sulfur into stable potassium-sulfur compound, such as K_2SO_4 . K_2/S equals one means that potassium and sulfur are in a stoichiometric amount, and are able to react completely, provided there are no potassium losses. There is another advantage to specify K_2/S ratios. When the percentage

of coal-bound sulfur is known, the amount of seed will be solely dependent on the amount of sulfur, or coal flow rate. Therefore, it skips the iteration processes usually needed if percent of potassium in total mass flow is specified. When K_2/S ratio is specified, M-COAL can still determine the percent of potassium in the total mass flow.

(3). A two stage combustion process is reflected by M-COAL. As mentioned in Chapter 1, CFFF operation consists of two stage combustion. The oxidant for primary combustion is oxygen-enriched air, while the oxidant for secondary combustion is just normal preheated air. Coal flow rate, the amount of potassium carbonate seed, primary stoichiometric ratio, etc., are all primary combustion parameters. Consequently, these parameters need to be determined separately from the amount of secondary air. M-COAL reads in two stoichiometric ratios: primary ratio (SR1) and secondary ratio (SR2)(defined in the following section). It then calculates the amount of primary oxygen-enriched air and secondary preheated air, respectively.

(4). The effect of potassium-slag interaction is taken into account. It has been recognized that combustion slag has a great affinity to potassium. Some 10-20 %(wt) K_2O has been detected in the slag samples collected at UTSI. They are usually in the form of stable melts, such as K_2SiO_3 , $K_2Si_2O_5$, or $KAlSi_nO_{2n+2}$ ($n = 0, 1, 2, \dots$) [6]. To deal with this part of potassium loss, real slag samples (test series LMF4-S, LMF4-T, LMF4-U) were collected and analyzed. Total amount of slag in a whole test was weighed. This value is divided by the total on-coal test time to give the slag removal rate during that test. The amount of K_2O interacted with slag is subtracted from the total potassium input. M-COAL then splits the seed (K_2CO_3) into two parts: $K_2O(s)$ and $CO_2(g)$. It is only the $K_2O(s)$ part of the input seed that is adjusted to account for the K_2O lost with slag.

In addition to four major modifications described above, M-COAL has its own self-explanatory input form. The input part that originally deals with the CHAN code or SYSTEM code is deleted (easily added if necessary), making M-COAL program especially suitable for modeling calculations of the process at CFFF.

2.4 Parameter Determination

In tests conducted at CFFF, several performance parameters such as coal flow rate, K_2/S ratio, primary stoichiometric ratio(SR1), secondary stoichiometric ratio(SR2), etc., are commonly adjusted to control the operating conditions. Typical operating conditions are shown in Table I and Table II.

Table I. Typical Operating Conditions at Primary Combustor

Parameter	Value
Peak Temperature (K)	3000
Pressure (atm)	4.5
Stoichiometric Ratio	0.85
K_2/S (molar ratio)	0.75–1.30
Coal/seed/moisture(kg/sec)	0.40*
Fuel oil(kg/sec)	0.19
Air(kg/sec)	1.56
O ₂ (kg/sec)	0.84
Upstream Purge N ₂ (kg/sec)	0.022

*Where Coal: 86 %; Seed(K_2CO_3): 11 %; Moisture: 3 %

Source: Individual Run Schedule for CFFF Test LMF4-R

Table II. Typical Operating Conditions at Secondary Combustor

Parameter	Value
Peak Temperature(K)	1500
Pressure (atm)	1.0
Secondary Air(kg/sec)	1.22
Secondary Air Temperature(K)	590
Residence Time(sec)	0.8
K ₂ /S Ratio	0.75–1.30
Downstream Purge N ₂ (kg/sec)	0.19

Source: Individual Run Schedule for Test LMF4-R

Corresponding to these performance parameters, K₂/S ratio, primary and secondary stoichiometric ratio, are chosen as modeling parameters. Combustion temperature is closely related to the coal flow rate and stoichiometric ratio. Presumably it is also one of the most important factors affecting the potassium-sulfur chemistry. Thus temperature is chosen as another modeling parameter. These parameters and their ranges are discussed in the following paragraphs.

Other variations, such as coal and fuel oil types, inclusion of new thermodynamic data, potassium loss in the slag, system purge nitrogen, etc. are also discussed in the following paragraphs. These variations are also expected to affect the results of the modeling calculations.

(1). Coal and Ash Analysis: Illinois No. 6 coal is used during LMF4 series tests. In order to closely model the test performance, actual coal analysis data from the test were used as input to M-COAL. Table III shows the coal and ash analysis data. This coal was used in the test LMF4-R(test data: Aug. 16 to Aug. 31, 1989).

Table III. Coal and Ash Analysis for Test LMF4-R

Proximate and Ultimate Analysis		Coal Ash Analysis	Wt %
Carbon (wt %)	70.40	SiO ₂	48.52
Hydrogen (wt %)	4.95	Al ₂ O ₃	21.37
Nitrogen (wt %)	1.28	Fe ₂ O ₃	13.57
Sulfur (wt %)	2.59	TiO ₂	0.69
Moisture (wt %)	3.38	CaO	3.68
Ash (wt %)	9.47	MgO	0.89
Heating Value (J/kg)	2.6498 ×10 ⁷	Na ₂ O	0.49
Chlorine (ppm)	2200	K ₂ O	5.07
		SO ₃	2.86

Source: Reported by Chem Lab at UTSI

(2). Oil Analysis: Fuel oil No. 2 is used during LMF4 series tests. Actual oil analysis data were also used as input to M-COAL. Table IV shows a typical fuel oil analysis data. The same oil was used in test LMF4-R.

Table IV. Fuel Oil Analysis for Test LMF4-R

Component	Wt (%)
Carbon	86.89
Hydrogen	12.92
Nitrogen	0.15
Sulfur	0.17
Heating Value J/kg	4.6287 ×10 ⁷

Source: Reported by Chem Lab at UTSI

During the tests, fuel oil was used in vitiation heater and primary combustor. Total oil flow is the summation of oil flow at these two locations. The average flow rates read from the entire LMF4-R test were 0.138 lb/sec at vitiation heater, and 0.298 lb/sec at primary combustor. The total oil flow rate is divided by the coal flow rate(0.896 lb/sec, of which seed %=12.19 %, and moisture=3.38 %), giving the ratio of oil-to-coal, ROC=0.577. This is also an input parameter for M-COAL.

(3). Temperature: Two temperature ranges are chosen in calculation. Temperature is varied from 2300 to 1100 K with 100 K difference for each step before secondary combustion. It varies from 1700 to 500 K with also 100 K difference for each step after secondary combustion. These two ranges cover the temperature measured from radiant furnace down to the air heater at CFFF.

(4). K₂/S Ratio: A wide range of K₂/S molar ratio is chosen. They are: K₂/S = 0.75, 1.00, 1.25, 1.50, 2.00. During the recent tests, K₂/S equals one is most commonly used as one of the parameters specified at stable operating condition. To investigate the impact of K₂/S ratio on downstream chemistry, K₂/S ratio greater or less than one is also used during some tests. This given range covers the operating conditions with respect to K₂/S ratio.

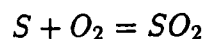
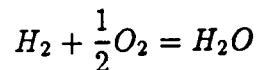
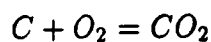
Most of the previous calculations in literature specified the amount of potassium input as the percentage of total mass flow at primary combustor. Usually 1 % K of total flow was the choice. As is known, K₂/S ratio is not directly related to the percentage of potassium in the total mass flow. Total mass flow depends on primary stoichiometric ratio, oxidizer, fuel oil flow, seed flow, as well as coal flow, while K₂/S ratio only depends on coal flow and sulfur content of the coal. If primary stoichiometric ratio (SR1) is 0.85, oil-to-coal weight ratio(ROC) is 0.577, oxygen-enriched air contains 40 % (volume) oxygen, and sulfur content of the

coal is 2.59% (from Table III), K_2/S ratio is 1.45 at 1% K of total mass flow.

(5). Stoichiometric Ratio: The stoichiometric ratio of oxygen in a combustion process is defined as the weight ratio of oxygen actually used to oxygen theoretically needed to convert the combustible elements contained in the fuel into their stable oxides.

$$SR = \frac{(O_2)_{actual}}{(O_2)_{theoretical}}$$

For a process utilizing coal and oil combustion, the amount of oxygen theoretically needed could be calculated from the following reaction equations:



The flow rate (by weight) of combustible elements, ie. C, H, S, can be obtained from coal analysis, fuel oil analysis, and coal and oil flow rates. Then the theoretical amounts of oxygen needed can be calculated from these number according to the above reactions. By specifying the stoichiometric ratio, the actual amount of oxygen can thus be obtained.

The primary stoichiometric ratio is the stoichiometric ratio as defined above for the primary combustion. The secondary stoichiometric ratio is actually the overall stoichiometric ratio. It is defined as the weight ratio of oxygen actually used in primary and secondary combustion to oxygen theoretically needed.

At CFFF, SR1 is almost always less than one, making the primary combustion under reducing conditions. SR2 is always greater than one, making the secondary combustion under oxidizing conditions. In the calculations, SR1 is

specified as: 0.80, 0.85, 0.90, 0.95, 1.00. SR2 is specified as: 1.05, 1.10, 1.15, 1.20.

(6). Inclusion of Thermodynamic Data: Thermodynamic properties of some important species expected in the MHD system were included in the data base of NASA code. These are of K_2SO_4 [7], KS, and K_2S [8].

The situation about condensed slag species is more complicated. Thermodynamic data for the condensed species, such as kyanite, kaolinite, $K_2O-4SiO_2-A$, $K_2O-4SiO_2-B$, $K_2Al_2Si_2O_8(s)$, $K_2Al_2Si_4O_{12}(s)$, $K_2Al_2Si_6O_{16}(l)$, etc., [9] were once included. This inclusion brought serious convergence problem. At all the conditions tried, only $K_2Al_2Si_6O_{16}(l)$ was discovered in the outputs. Its molar fraction was also very small. Therefore, these condensed species data are not included in the present calculations.

(7). Potassium Losses to Slag: To calculate the amount of potassium lost to slag, one needs to know the composition of potassium in the slag and the percentage of slag removal. Table V gives four sets of slag analysis data for tests LMF4-R, S, T, and U, reported by the Chem Lab at UTSI.

To find out the percentage of slag removal, one needs to know the total amount of slag formed/collected, total on-coal time for a particular test, and the ash input. Table VI gives this information.

Table V. Slag Analysis for Recent LMF4 Tests

Parameter	Value (wt %)			
	LMF4-R	LMF4-S	LMF4-T	LMF4-U
Test Number				
Test Time(hr)	262.61	134.63	223.10	251.55
SiO ₂	9.23	39.72	48.92	45.07
Al ₂ O ₃	16.90	21.81	16.78	19.36
Fe ₂ O ₃	11.44	9.83	11.12	10.76
TiO ₂	0.86	0.87	0.96	0.54
CaO	3.29	3.46	3.31	3.19
MgO	0.82	0.79	0.81	0.84
Na ₂ O	0.35	0.33	0.47	0.39
K ₂ O	17.25	18.34	18.52	17.99
SO ₃	0.05	0.25	0.05	0.46

Source: Reported by Chem Lab at UTSI

Table VI. Slag Removal at Radiant Furnace

Test Number	Time(hr)	Ash Input(lbs)	Slag(lbs*)	Slag Removed %
LMF4-I	70.12	21,708	18,312	84.4
LMF4-K	198.33	65,385	47,889	73.2
LMF4-N	179.07	62,476	51,830	82.9
LMF4-O	252.38	113,888	65,497	57.5
LMF4-P	101.32	44,201	27,647	62.5
LMF4-R	262.61	72,874	53,253	73.1
LMF4-S	134.63	36,942	30,936	83.7

*Source: Data from D. Jackson's Mass Balance Work

The average coal ash removal as slag at Radiant Furnace(RF) is about 73.9% of the total coal ash input. In the subsequent equilibrium calculations, the percentage of slag removal at RF is specified to be 70 %.

When preparing the input to the NASA code, the total amount of seed(K_2CO_3) is calculated by M-COAL first, according to the coal and fuel oil analyses and specified K_2/S ratio. Then the seed ($K_2CO_3(s)$) is divided into two parts, $CO_2(g)$ as calculated, and $K_2O(s)$, which is the originally calculated value subtracted by about 10 %(wt) of that value considered as tied up in the slag. Appendix A gives an example showing this calculation in detail.

(8). Purge Nitrogen: Throughout the CFFF, purge nitrogen is used to prevent the instruments from plugging. Although this part of nitrogen is believed not to react with other elements or species in the system, its input does affect the molar fractions of the final species. During the tests, purge nitrogen is classified into two categories: upstream purge nitrogen and downstream purge nitrogen.

In the calculations, two values of purge nitrogen are chosen corresponding to Secondary Combustor Inlet(SCI) and Secondary Combustor Outlet(SCO) location. Based on past experiences, purge nitrogen is specified as 40 lb/100 lb coal input before the secondary combustion, and 60 lb/100 lb coal after the secondary combustion.

CHAPTER 3

CALCULATED RESULTS AND INTERPRETATIONS

3.1 Potassium and Sulfur Species at Equilibrium

Based on modifications to the NASA code and COAL code and determinations of the parameters described in the previous chapter, extensive parametric calculations were carried out. The following four tables list most of the potassium and sulfur species calculated to exist at equilibrium under typical CFFF operating conditions. Table VII and IX list the species expected before secondary combustion. The parameters chosen are $K_2/S=1.25$, and $SR1=0.85$. Table VIII and X list the species expected after secondary combustion, the parameters chosen are $K_2/S=1.25$, $SR1=0.85$, and $SR2=1.10$. It should be noted that the species in gas phase are listed just by their molecular formulae, while the species in condensed phase are listed by their molecular formulae followed by parentheses, in which the state of the species is also shown. For example, K_2SO_4 represents gas phase potassium sulfate, whereas $K_2SO_4(l)$, $K_2SO_4(s)$, and $K_2SO_4(c)$ represent liquid, solid and condensed state of potassium sulfate, respectively.

**Table VII. Molar Fraction of Potassium Species before
Secondary Combustion ($K_2/S=1.25$, $SR1=0.85$)**

Species	Molar Percentage (%)						
	2300 K	2200 K	2100 K	1800 K	1500 K	1400 K	1300 K
K	50.24	46.75	43.09	23.28	12.67	9.39	5.47
KO	0.14	0.07	0.03	0.00	0.00	0.00	0.00
KOH	49.58	53.14	56.84	52.61	62.63	65.11	55.85
KH	0.04	0.03	0.03	0.01	0.01	0.00	0.00
K ₂ CO ₃ (l)	0.00	0.00	0.00	0.00	0.00	0.00	12.56
K ₂ O ₂ H ₂	0.00	0.00	0.00	0.00	0.02	0.07	0.20
K ₂ SO ₄	0.00	0.00	0.00	0.00	0.03	0.05	0.04
KS	0.00	0.00	0.01	0.03	0.08	0.06	0.03
K ₂ S	0.00	0.00	0.00	0.01	0.49	1.24	1.77
K ₂ SiO ₃ (l)	0.00	0.00	0.00	24.08	24.08	24.08	24.08

**Table VIII. Molar Fraction of Potassium Species after
Secondary Combustion ($K_2/S=1.25$, $SR1=0.85$, $SR2=1.10$)**

Species	Molar Percentage (%)						
	1700 K	1600 K	1500 K	1400 K	1300 K	800 K	500 K
K	0.84	0.27	0.03	0.00	0.00	0.00	0.00
KO	0.02	0.01	0.00	0.00	0.00	0.00	0.00
KOH	71.43	55.06	13.21	2.44	0.81	0.00	0.00
K ₂ CO ₃ (s)	0.00	0.00	0.00	0.00	0.00	0.00	14.55
K ₂ O ₂ H ₂	0.00	0.01	0.00	0.00	0.00	0.00	0.00
K ₂ SO ₄	3.62	20.58	6.98	1.69	0.29	0.00	0.00
K ₂ SO ₄ (s)	0.00	0.00	0.00	0.00	0.00	85.45	85.45
K ₂ SO ₄ (s)	0.00	0.00	0.00	0.00	84.92	0.00	0.00
K ₂ SO ₄ (l)	0.00	0.00	55.70	77.43	0.00	0.00	0.00
K ₂ SiO ₃ (s)	0.00	0.00	0.00	0.00	0.00	14.55	0.00
K ₂ SiO ₃ (l)	24.09	24.08	24.08	18.43	13.98	0.00	0.00

**Table IX. Molar Fraction of Sulfur Species before
Secondary Combustion ($K_2/S=1.25$, $SR1=0.85$)**

Species	Molar Percentage (%)						
	2300 K	2200 K	2100 K	1800 K	1500 K	1400 K	1300 K
SO ₂	92.39	92.83	93.14	90.31	31.57	9.43	1.65
COS	0.01	0.02	0.04	0.49	5.31	6.89	6.76
CAS(s)	0.00	0.00	0.00	0.00	2.29	2.29	2.29
H ₂ S	0.05	0.09	0.19	3.10	47.92	72.18	84.67
K ₂ SO ₄	0.00	0.00	0.00	0.00	0.03	0.05	0.05
KS	0.01	0.01	0.01	0.06	0.19	0.14	0.06
K ₂ S	0.00	0.00	0.00	0.01	0.57	1.45	2.07
S	0.15	0.14	0.13	0.09	0.02	0.00	0.00
SH	0.12	0.15	0.20	0.57	0.82	0.45	0.16
SN	0.01	0.00	0.00	0.00	0.00	0.00	0.00
SO	7.27	6.75	6.26	4.62	1.05	0.26	0.04
SO ₃	0.01	0.00	0.00	0.00	0.00	0.00	0.00
S ₂	0.00	0.01	0.02	0.72	10.09	6.80	2.24
S ₂ O	0.00	0.00	0.00	0.03	0.14	0.06	0.01

**Table X. Molar Fraction of Sulfur Species after Secondary
Combustion ($K_2/S=1.25$, $SR1=0.85$, $SR2=1.10$)**

Species	Molar Percentage (%)						
	1700 K	1600 K	1500 K	1400 K	1300 K	800 K	500 K
SO ₂	95.55	75.67	26.50	7.32	0.27	0.00	0.00
K ₂ SO ₄	4.24	24.08	8.17	1.98	0.34	0.00	0.00
K ₂ SO ₄ (s)	0.00	0.00	0.00	0.00	0.00	100.00	100.00
K ₂ SO ₄ (s)	0.00	0.00	0.00	0.00	99.37	0.00	0.00
K ₂ SO ₄ (l)	0.00	0.00	65.18	90.62	0.00	0.00	0.00
Na ₂ SO ₄	0.00	0.00	0.00	0.01	0.02	0.00	0.00
SO	0.00	0.00	0.00	0.00	0.00	0.00	0.00
SO ₃	0.21	0.25	0.14	0.07	0.01	0.00	0.00

Table VII shows that the major potassium species before secondary combustion are K, KOH, $K_2SiO_3(l,s)$, and if temperature is low enough then $K_2CO_3(l,s)$. Table VIII shows that the major potassium species after secondary combustion are $K_2SO_4(s)$, and $K_2SiO_3(s)$. If temperature is high enough, KOH and K_2SO_4 also exist. If temperature is low enough, all the $K_2SiO_3(s)$ may convert to $K_2CO_3(s)$.

The major sulfur species before secondary combustion, according to Table IX, are SO_2 and H_2S , although SO, S_2 , COS together also comprise a significant part of the total sulfur species. After secondary combustion, major sulfur species, according to Table X, are K_2SO_4 and $K_2SO_4(l,s)$. SO_2 concentration drops very quickly as gas temperature decreases.

These major species, namely SO_2 , H_2S , K, KOH, $K_2SO_4(l,s)$, $K_2CO_3(l,s)$, and $K_2SiO_3(l,s)$, consist more than 90 % (by mole) of the total sulfur or potassium species. Therefore, the following sections are used mainly to investigate their interactions and transformations, and how various factors in operation, i.e. temperature, stoichiometric ratios, potassium-to-sulfur ratio, etc., affect such interactions and transformations.

On the other hand, there are also some minor sulfur species, such as SO, S_2 , and COS. Although their total amount is usually less than 10 % (sometimes higher), they play an important role in the kinetics of potassium-sulfur interactions. Therefore, the effects of such minor sulfur species on potassium-sulfur interactions are also investigated in the following sections. Besides, thermodynamic data of several potassium compounds, such as K_2SO_4 , KS, K_2S are first time included in the NASA data base. The results due to the inclusion of these data deserve specific attention and are discussed in the following sections.

3.2 SO₂ and H₂S Behavior before Secondary Combustion

3.2.1 SO₂ and H₂S Behavior with respect to Gas Temperature

Figure 3-1 shows the relationship between the molar percentage of total sulfur species as SO₂ or H₂S and gas phase temperature. SR1 is 0.85 and K₂/S ratio is 1.25.

It can be seen that temperature is a very important factor in certain region. From 2300 to 1800 K, SO₂ consists about 92 % (by mole) of the total sulfur species. It experiences a small local maximum (at about 2000 K), but remains almost unchanged throughout this range. H₂S, in this temperature region, is of low concentration. When temperature drops below 1800 K, SO₂ concentration decreases quickly while H₂S concentration increases at the same speed. In fact, the figure looks symmetric, which means that all SO₂ is converted to H₂S. At about 1530 K, SO₂ and H₂S have the same concentration, each of them consists about 40 % of the total sulfur species. At 1400 K, which is about the temperature of secondary combustor inlet, SO₂ consists only about 10 %, while H₂S is about 70 % of the total sulfur species. It shows that most of the sulfur species are in reduced forms at SCI, giving the same results as one should have expected.

Temperature below 1400 K is a hypothetical situation, because at this point, preheated air is introduced into secondary combustor at CFFF, and the entire operating condition is changed from reducing to oxidizing. However, it is still helpful to look into the behavior of sulfur species below this temperature. The results of calculations below 1400 K can be used to explain the possible reaction taking place in the sampling probe, where the temperature could decrease from that of the sampling point to several hundred degrees(K).

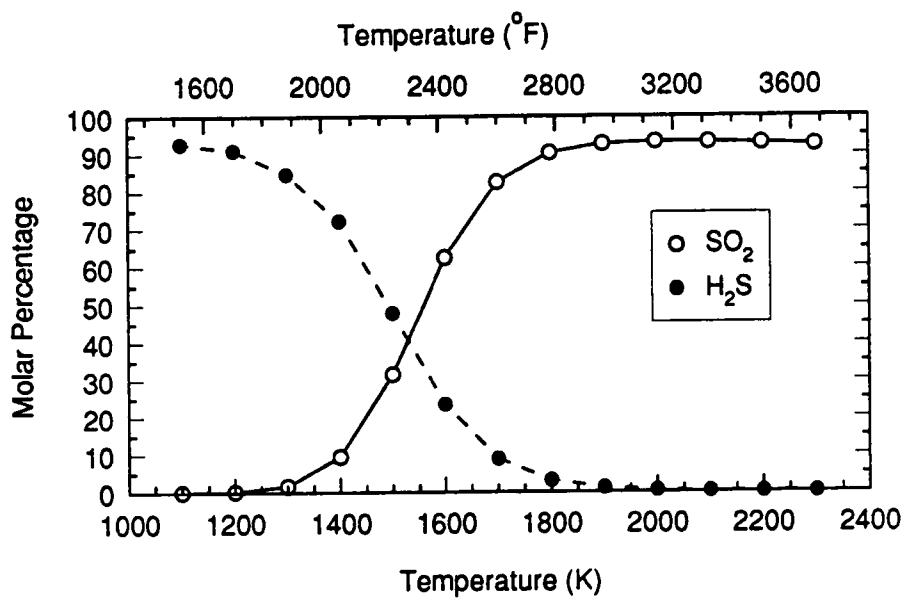


Figure 3-1. Fraction of Total Sulfur Species as SO₂ or H₂S vs. Temperature (K₂/S=1.25,SR1=0.85)

3.2.2 SO₂ and H₂S Behavior with respect to K₂/S Ratio

Figure 3-2 shows the relationship between molar percentage of total sulfur species as SO₂ or H₂S and temperature at different K₂/S ratios. Primary stoichiometric ratio used is 0.85. Figure 3-2 looks similar to Figure 3-1. It is clear from the figure that K₂/S ratio (from 0.75 to 2.00) has no effect on the concentration of SO₂. K₂/S ratio does affect the concentration of H₂S a little, especially at temperatures around 1400 K. However, the effect of K₂/S ratio on H₂S is so small that it can also be neglected.

3.2.3 SO₂ and H₂S Behavior with respect to Primary Stoichiometric Ratio

Figure 3-3 shows the relationship between molar percentage of total sulfur species as SO₂ and temperature at different primary stoichiometric ratios. K₂/S ratio used is 1.0. This figure has the same trend as Figures 3-1 and 3-2. In high temperature region (2300–1800 K), SO₂ concentration remains almost unchanged. At slightly low temperatures (1800–1400 K), SO₂ concentration drops very quickly. At low temperatures (below 1400 K), SO₂ concentration is very low, and almost zero.

An interesting point is, if primary stoichiometric ratio rises by 0.05, the temperature at which SO₂ concentration remains the same decreases by about 100 K. For example, if SO₂% stays at 60%, then

$$SR1 = 0.80, \quad T = 1700 \text{ K}$$

$$SR1 = 0.85, \quad T = 1600 \text{ K}$$

$$SR1 = 0.90, \quad T = 1500 \text{ K}$$

The higher the stoichiometric ratio, the higher is the concentration of SO₂, if temperature remains the same. Differences in SO₂ concentration due to different stoichiometric ratios change a lot at different temperatures. They range from

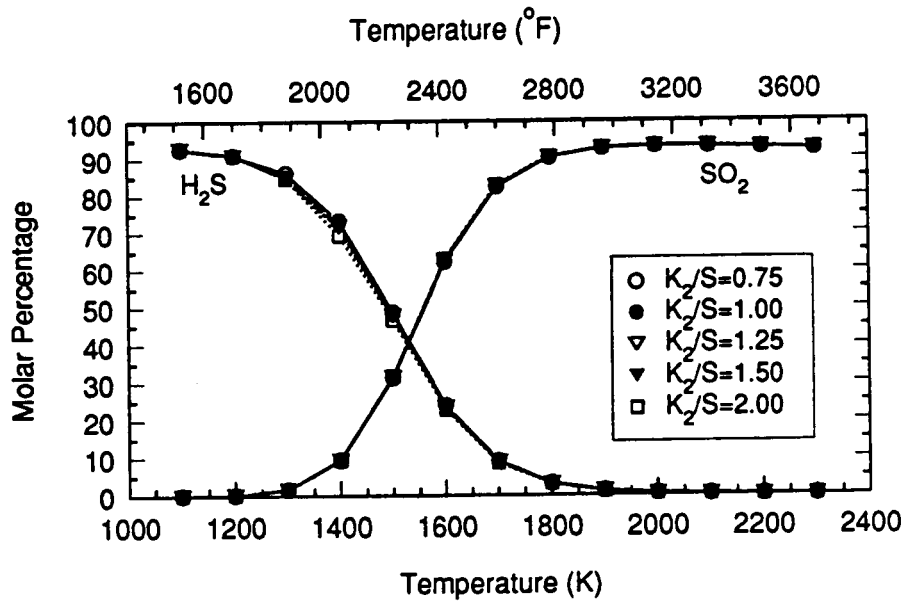


Figure 3-2. Fraction of Total Sulfur Species as SO_2 or H_2S vs. Temperature at Different K_2/S Ratios ($\text{SR1}=0.85$)

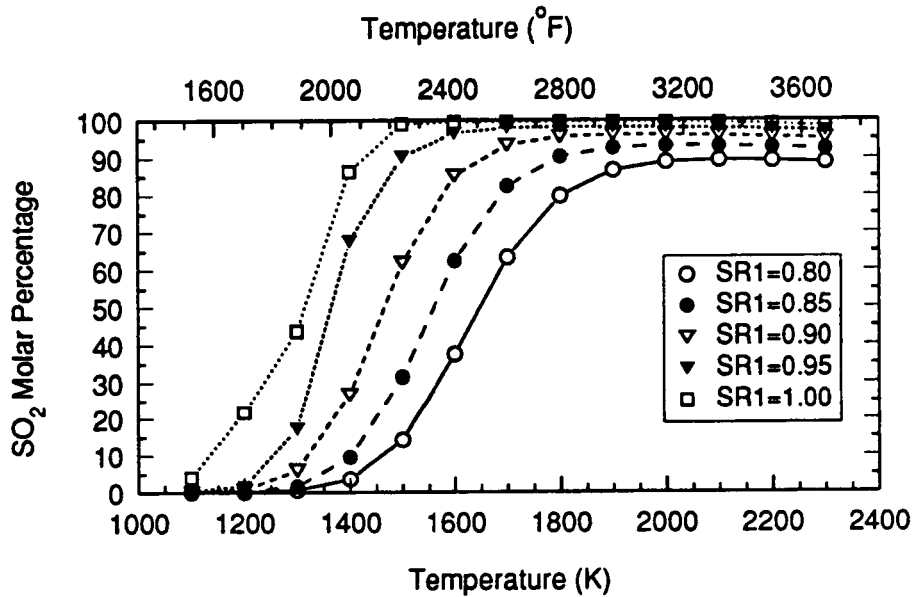


Figure 3-3. Fraction of Total Sulfur Species as SO_2 vs. Temperature at Different SR1 ($K_2/S=1.00$)

about 5 % (at high temperature) to about 40 % (at medium temperature). For example,

	T = 2200 K	T = 1400 K
SR1 = 0.80	SO ₂ % = 87 %	SO ₂ % = 4 %
SR1 = 0.85	SO ₂ % = 92 %	SO ₂ % = 10 %
SR1 = 0.90	SO ₂ % = 95 %	SO ₂ % = 26 %

Figure 3-4 shows the relationship between molar percentage of H₂S and temperature at different primary stoichiometric ratios. This figure also has the similar trend as Figures 3-1 and 3-2. Several interesting points can be seen here too. First, if temperature is low enough, H₂S molar percentage tends to be the same at different stoichiometric ratios. Second, at medium temperature, if stoichiometric ratio rises by 0.05, the temperature of equal H₂S concentration decreases by about 100 K. For example, if H₂S% stays at 20%, then

SR1 = 0.80,	T = 1700 K,
SR1 = 0.85,	T = 1600 K,
SR1 = 0.90,	T = 1500 K,
SR1 = 0.95,	T = 1400 K.

Third, at a specified temperature, the lower the stoichiometric ratio, the higher is the H₂S concentration.

3.3 SO₂ Behavior after Secondary Combustion

3.3.1 SO₂ Behavior with respect to Secondary Stoichiometric Ratio

Figure 3-5 shows the relationship between the molar fraction of all the species as SO₂ and gas temperature at different secondary stoichiometry ratios. K₂/S ratio used is 1.0.

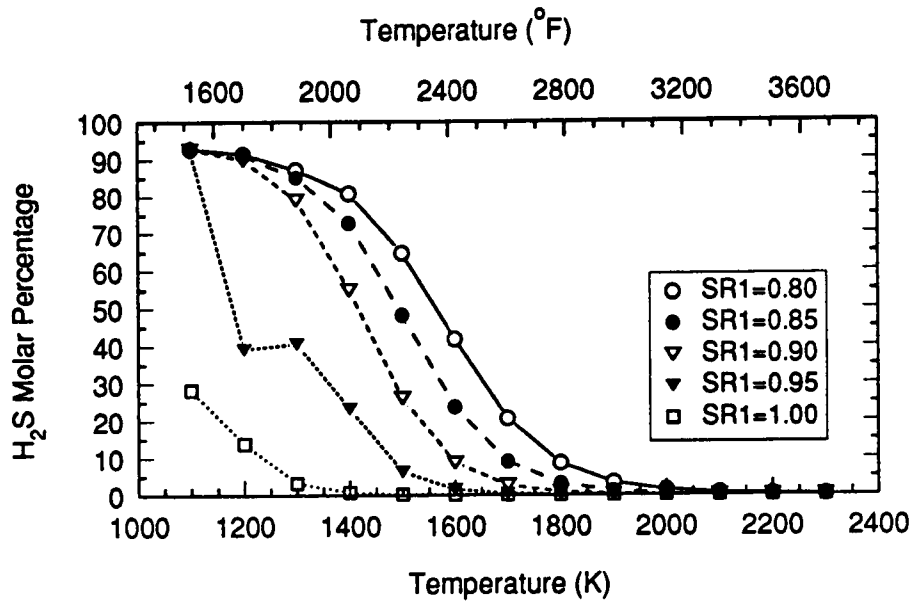


Figure 3-4. Fraction of Total Sulfur Species as H_2S vs. Temperature at Different SR1 ($K_2/S=1.00$)

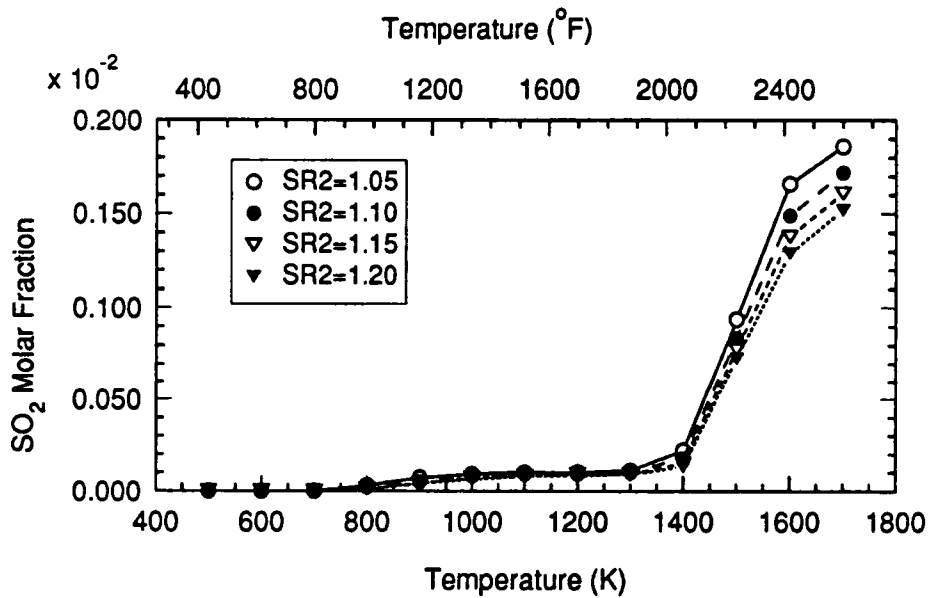


Figure 3-5. Fraction of Total Sulfur Species as SO_2 vs. Temperature at Different SR2 ($K_2/S=1.00, SR1=0.85$)

It is clear that SO_2 is very sensitive to temperature in 1600 - 1400 K range. SO_2 concentration drops from about 1700 ppm to about 200 ppm in this temperature region. This is where secondary combustion at CFFF is carried out. So it is not surprising that most of the conversion reactions involving sulfur species are completed in this region. When temperature decreases further, SO_2 concentration becomes very small (100 ppm). If temperature is below 800 K, SO_2 concentration is almost zero, according to this figure.

Another interesting point is that secondary stoichiometric ratio (or overall stoichiometric ratio) does not affect SO_2 concentration very much at low temperature. Four lines which represent the secondary stoichiometric ratio from 1.05 to 1.20 are very close to each other below 1400 K.

However, it is probably true that the effects of secondary stoichiometric ratio varies at different level of SR2. They are more significant for $\text{SR2} < 1.10$. This phenomenon is evident in Figure 3-5, but better shown in Figure 3-6.

In Figure 3-6, three lines, representing $\text{SR2}=1.10$, 1.15, and 1.20, are very close to each other. While the line which represents $\text{SR2}=1.05$ is apart from the line of $\text{SR2}=1.10$. In terms of SO_2 concentration, there is about 100 ppm or more drop when stoichiometric ratio increases from 1.05 to 1.10. After that, SO_2 concentration drops only about 20 ppm or less for each 0.05 increase of stoichiometric ratio. When temperature is below 1200 K, SO_2 concentration is essentially zero. It should be noted that K_2/S ratio in Figure 3-6 is 1.25.

3.3.2. SO_2 Concentration with Respect to K_2/S Ratio

Figure 3-7 shows the relationship between the molar fraction of all the species as SO_2 and gas temperature at different K_2/S ratios. Stoichiometric ratio used is 1.05.

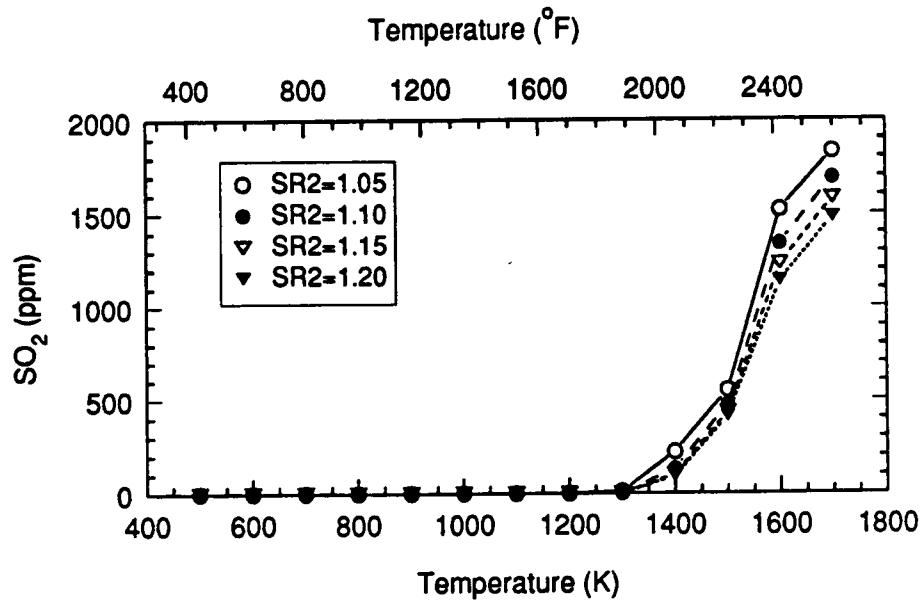


Figure 3-6. Fraction of Total Sulfur Species as SO_2 vs. Temperature at Different SR_2 ($K_2/S=1.25, \text{SR}_1=0.85$)

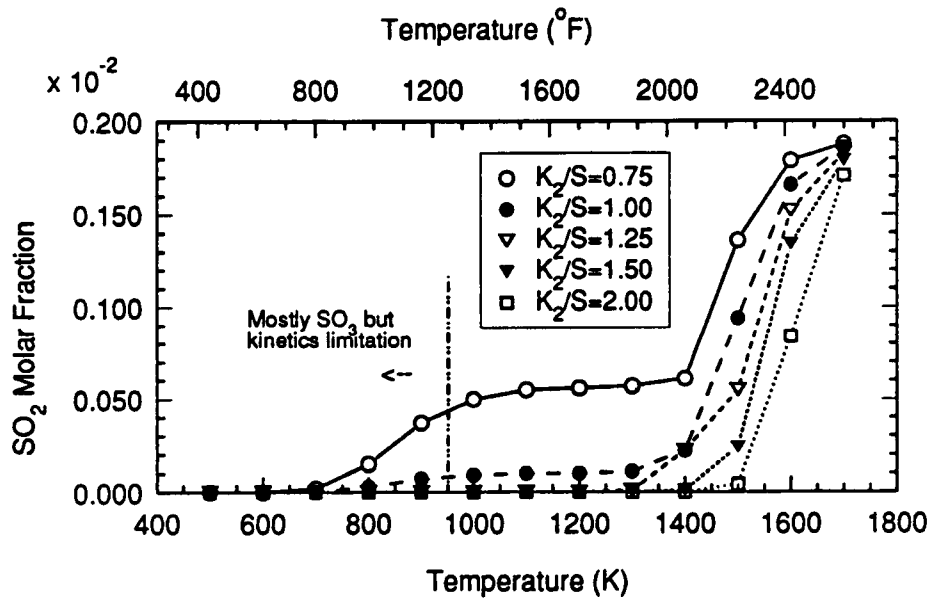
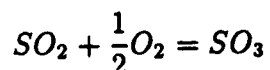


Figure 3-7. SO_2 Concentrations (wet basis) vs. Temperature at Different K_2/S Ratios ($\text{SR}_2=1.05$)

This figure shows that K_2/S ratio has a profound effect on SO_2 concentration after secondary combustion. As mentioned in the previous section, most of the SO_2 conversion reactions occur and are almost completed between 1600 - 1400 K. However, if $K_2/S < 1$, SO_2 conversion reaction is not complete. There is a significant amount of SO_2 gas remaining between 1000 - 1400 K, and it remains unchanged around 600 ppm. Between 700 - 1000 K, there is a relatively small change in SO_2 concentration. Below 700 K, SO_2 concentration drops to zero. Here the SO_2 has most likely converted to SO_3 according to equilibrium calculation. Usually, the reaction



is favored thermodynamically at low temperature, but the reaction may be proceeding extremely slow without a proper catalyst.

If $K_2/S=1.0$, there is also a similar plateau in SO_2 concentration between 900 - 1300 K. The SO_2 concentration on the plateau is only about 100 ppm. Below 700 K, SO_2 concentration also becomes zero. If $K_2/S > 1$, there is no similar plateau in SO_2 concentration. Here the concentration of SO_2 drops down to zero very quickly.

It is also worthwhile to identify the temperature difference at the same SO_2 concentration, and the SO_2 concentration differences at the same temperature for different K_2/S ratios. When $K_2/S > 1$, the temperatures at which SO_2 concentration reaches zero are:

$$K_2/S = 1.25, \quad T = 1250 \text{ K,}$$

$$K_2/S = 1.50, \quad T = 1300 \text{ K,}$$

$$K_2/S = 2.00, \quad T = 1400 \text{ K.}$$

On the other hand, if $T = 1500 \text{ K}$, then

$$\begin{aligned}
 K_2/S &= 1.00, & [SO_2] &= 900 \text{ ppm}, \\
 K_2/S &= 1.25, & [SO_2] &= 600 \text{ ppm}, \\
 K_2/S &= 1.50, & [SO_2] &= 300 \text{ ppm}, \\
 K_2/S &= 2.00, & [SO_2] &= 30 \text{ ppm}.
 \end{aligned}$$

Since SO_2 is one of the major pollutant emissions in the CFFF system, its behavior with respect to gas temperature, K_2/S ratio, primary and secondary stoichiometric ratio, etc. should be fully investigated. In section 5.4, an empirical analytical equation concerning these parameters is presented.

3.4 Potassium Species Behavior before and after Secondary Combustion

As mentioned in the first section of this chapter, the major potassium species are K, KOH before secondary combustion, and KOH, $K_2SO_4(l,s)$ after secondary combustion. These major species are shown in Figures 3-8 and 3-9.

Figure 3-8 shows the relationship between molar percentage of selected potassium species (K, KOH, $K_2CO_3(c)$, $K_2SiO_3(s)$) and gas phase temperature before secondary combustion for $K_2/S=1.25$ and $SR1=0.85$. The concentration values of liquid and solid phases for a species(l,s) are combined together and then expressed as one concentration value of condensed phase for that particular species(c).

Figure 3-9 shows the relationship between molar percentage of major potassium species(KOH, K_2SO_4 , $K_2SO_4(c)$, $K_2CO_3(c)$, $K_2SiO_3(c)$) and gas temperature after secondary combustion for $K_2/S=1.25$, $SR1=0.85$, and $SR2=1.05$.

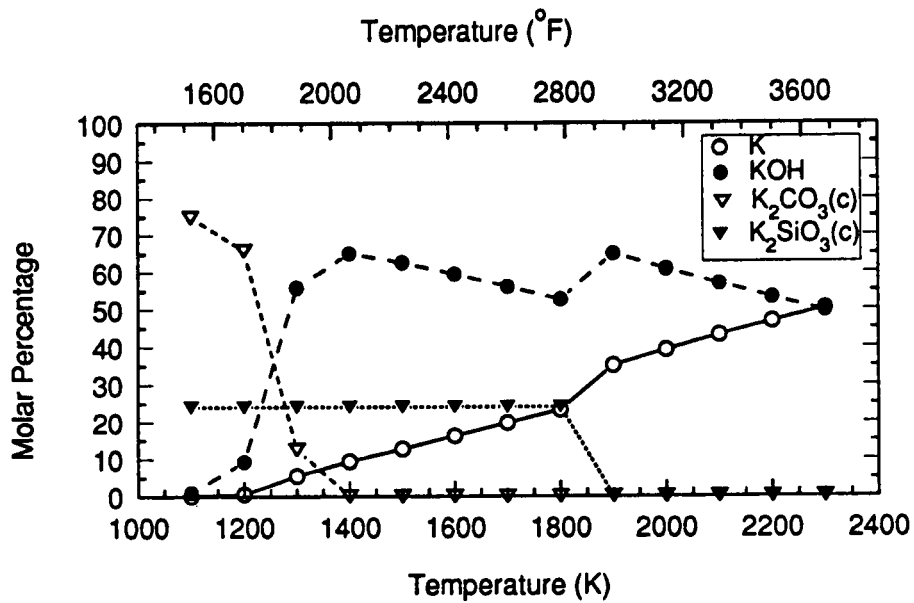


Figure 3-8. Fraction of Total Potassium Species as Major Potassium Species vs. Temperature before Secondary Combustion ($K_2/S=1.25, SR1=0.85$)

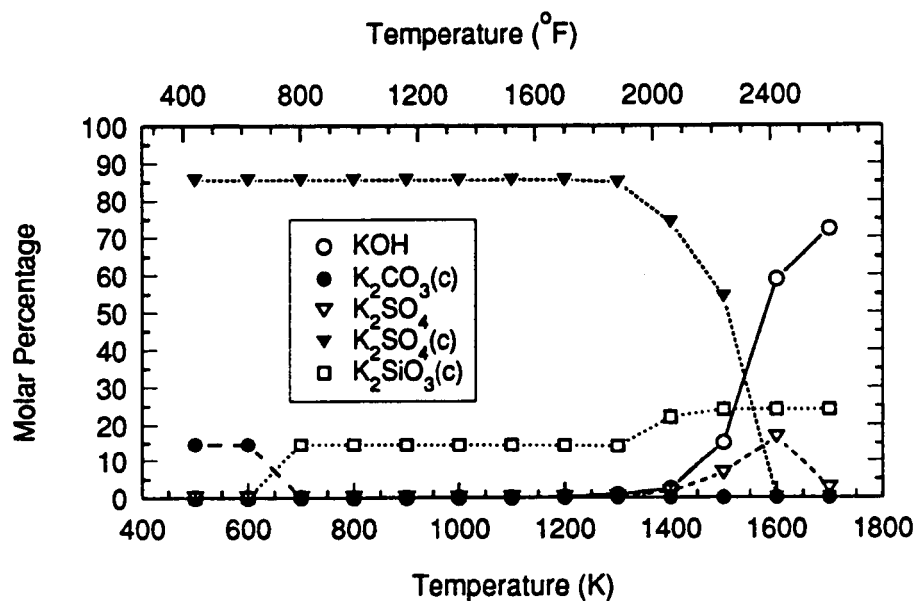


Figure 3-9. Fraction of Total Potassium Species as Major Potassium Species vs. Temperature after Secondary Combustion ($K_2/S=1.25, SR1=0.85, SR2=1.05$)

3.4.1. The Effect of SR1 on K, KOH before Secondary Combustion

Figures 3-10 and 3-11 show the effects of primary stoichiometric ratio on the molar percentage of K and KOH before secondary combustion for $K_2/S=1.25$.

Because of the formation of new potassium species or the phase transition for a particular potassium species, the slopes of the curves in figures 3-10 and 3-11 are discontinuous. At high temperature (2300–1900 K), K % decreases continuously, while KOH % increases at the same speed as temperature decreases. This means that K is solely converted to KOH during this region. This is also shown much clearly in Figure 3-8. At 1900 K, both the concentration of K and KOH have a sharp drop due to the formation of $K_2SiO_3(c)$. After $K_2SiO_3(c)$ reaches its equilibrium concentration, the same trend as at high temperature appears, i.e. K % decreases while KOH % increases continuously as temperature decreases. At low temperature (below 1400 K), new potassium species, such as $K_2CO_3(c)$ may form. Consequently, the concentration of K and KOH will experience a sharp drop. At sufficiently low temperature, the concentrations of K and KOH all become zero. Potassium will be then in the form of $K_2SiO_3(c)$ and $K_2CO_3(c)$.

The higher the primary stoichiometric ratio, the higher is the molar percentage of KOH, and the lower is the molar percentage of K. Under the conditions listed in Figure 3-8 ($K_2/S=1.25$, $SR1=0.85$) and high temperature, the percentage of K and KOH of total potassium species are about the same, i.e. 50 % to 50 %. Figure 3-10 shows that K % could be up to 60 % of the total potassium species. Figure 3-11 shows that KOH % could be up to 90 % of the total potassium species.

As is shown in Figures 3-10 and 3-11, primary stoichiometric ratio has bigger

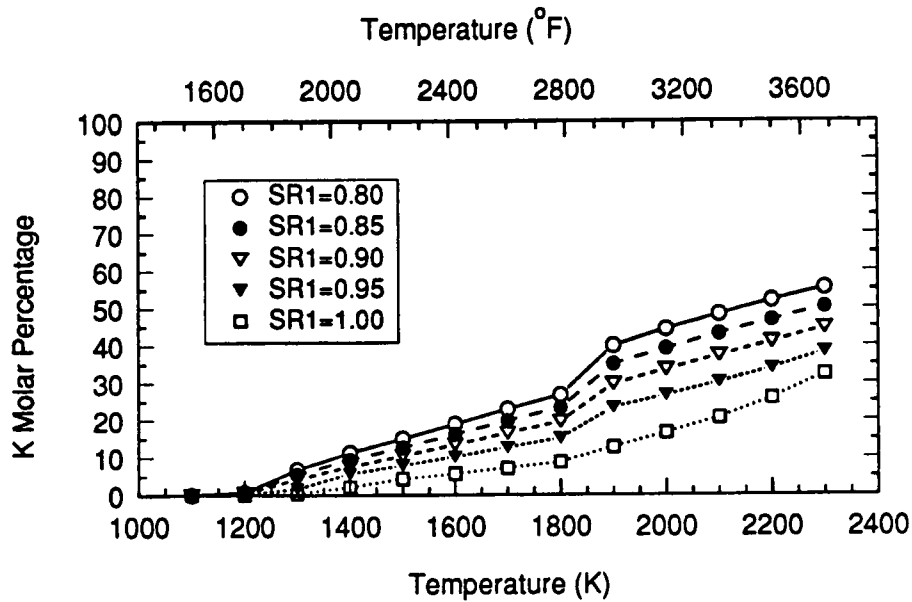


Figure 3-10. Fraction of Total Potassium Species as Gas Phase K vs. Temperature at Different SR1 ($K_2/S=1.25$)

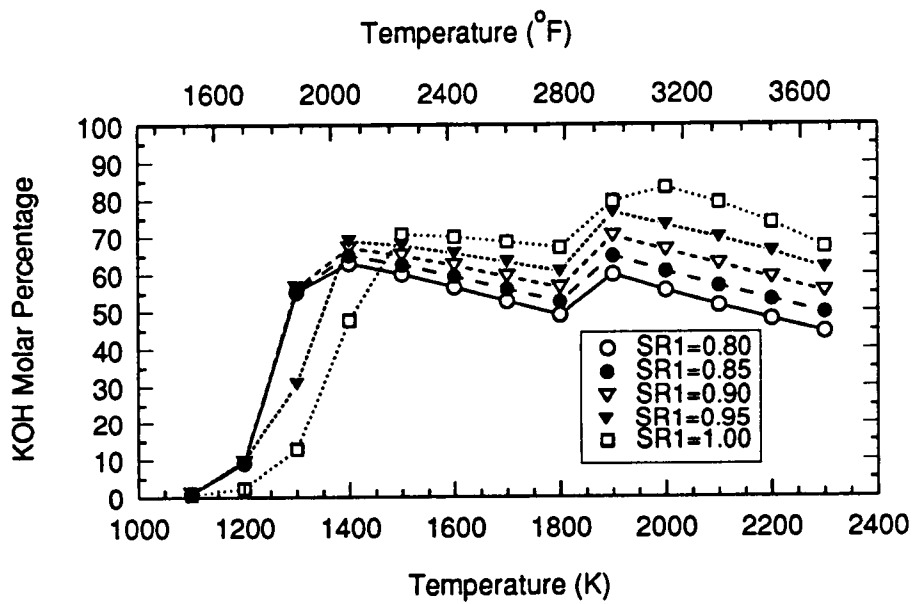


Figure 3-11. Fraction of Total Potassium Species as Gas Phase KOH vs. Temperature at Different SR1 ($K_2/S=1.25$)

impact on the concentration of K and KOH at higher temperatures than at lower ones. This is because at high temperature, K and KOH consist of almost all the potassium species. When temperature decreases, other forms of potassium species occur. Thus, the effects of stoichiometric ratio are shared by more species at low temperature than at high temperature. The difference in K % or KOH % based on a 0.05 step increase in primary stoichiometric ratio at high temperature is 5 - 10 %. This number decreases to 2 - 5 % at low temperature.

3.4.2. The Effect of K_2/S Ratio on K, KOH before Secondary Combustion

Figures 3-12 and 3-13 show the effects of K_2/S ratio on the concentration of K and KOH for $SR_1=0.85$.

It is clear that K_2/S ratio has no effect on the molar percentage of K and KOH at high temperature (2300–1900 K). At medium temperature (1400 - 1900 K), K_2/S ratio affects the molar percentage of KOH more than that of K. At low temperature (below 1300 K), the molar percentages of K and KOH both approach zero, K_2/S ratio has very little effect on them.

While at medium temperature, the impact of K_2/S ratio on the molar percentage of K and KOH still varies according to the value of K_2/S ratio. If $K_2/S < 1$, it has a relatively bigger impact on the molar percentage of K and KOH. If $K_2/S > 1$, it has a smaller impact on the molar percentage of K and KOH. After all, the effects of K_2/S ratio on the molar percentage of K and KOH are not significant.

The sharp drop point in the molar percentage of K and KOH also varies according to the K_2/S ratio. The smaller the K_2/S ratio, the lower the temperature at which a sharp drop in K % and KOH % occurs, which means that at lower temperature other potassium species, such as $K_2SiO_3(c)$ may be forming.

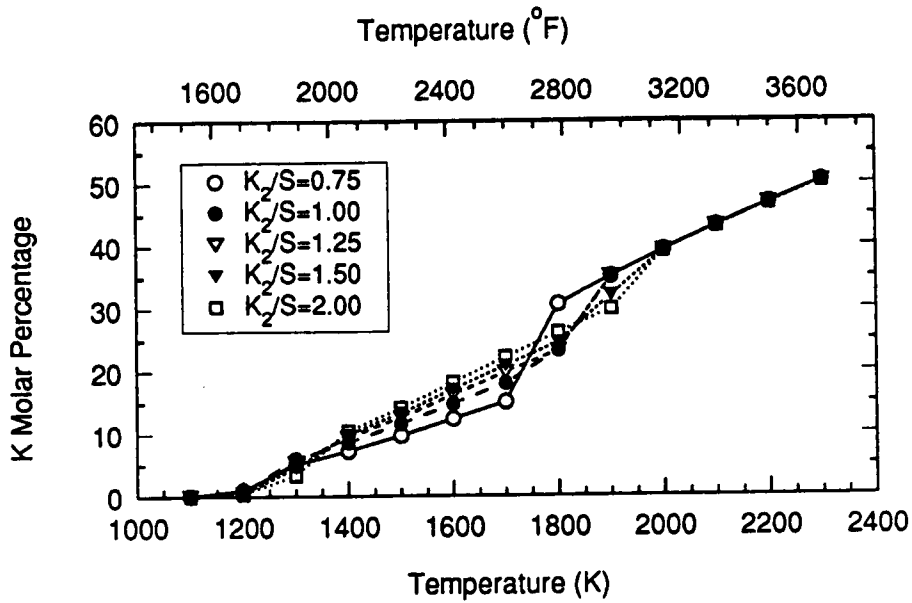


Figure 3-12. Fraction of Total Potassium Species as Gas Phase K vs. Temperature at Different K_2/S Ratios(SR1=0.85)

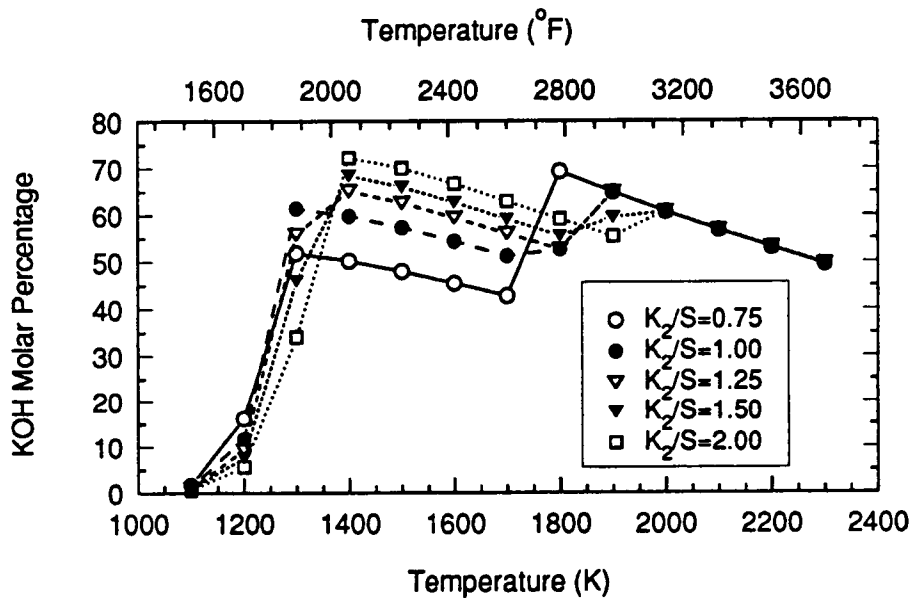


Figure 3-13. Fraction of Total Potassium Species as Gas Phase KOH vs. Temperature at Different K_2/S Ratios(SR1=0.85)

3.4.3. The Effect of K_2/S on KOH, $K_2SO_4(c)$ after Secondary Combustion

As is mentioned in the first section, the major potassium species after secondary combustion is $K_2SO_4(c)$. Other potassium species are KOH(1700 - 1400 K), $K_2SiO_3(c)$ (1700 - 700 K), and $K_2CO_3(c)$ (below 600 K). Figures 3-14 and 3-15 show the effect of K_2/S ratio on the molar percentages of $K_2SO_4(c)$ and KOH of total potassium species for $SR1=0.85$, and $SR2=1.05$.

In Figure 3-14, K_2SO_4 starts to condense when temperature is below 1600 K. It attains its equilibrium concentration quickly at about 1400 K. Then the percentage of $K_2SO_4(c)$ of total potassium species remains unchanged as temperature decreases further.

At $K_2/S \leq 1$, potassium species consist of almost 100 % $K_2SO_4(c)$. As K_2/S ratio increases, molar percentage of $K_2SO_4(c)$ decreases. For example, when K_2/S ratio increases from 1.0 to 1.25, molar percentage of $K_2SO_4(c)$ decreases from about 100 % to about 85 %. When K_2/S ratio increases from 1.25 to 1.50, molar percentage of $K_2SO_4(c)$ decreases from about 85 % to about 70 %. This means $K_2SO_4(c)$ is the most favorable product thermodynamically.

Figure 3-15 shows that if $K_2/S < 1.5$, K_2/S ratio has no effect on the molar percentage of KOH. If $K_2/S \geq 1.5$, however, there will be a plateau in the figure. When $K_2/S=1.5$, the plateau occurs between 1200 - 1400 K, and the molar percentage of KOH is about 10 %. When $K_2/S=2.0$, the plateau occurs between 1300 - 1500 K, and the molar percentage of KOH is about 35 %.

If $K_2/S < 1.5$, molar percentage of KOH experiences a sharp drop between 1400 - 1600 K. It approaches zero when temperature is below 1400 K. If $K_2/S \geq 1.5$, molar percentage of KOH approaches zero below 1100 K.

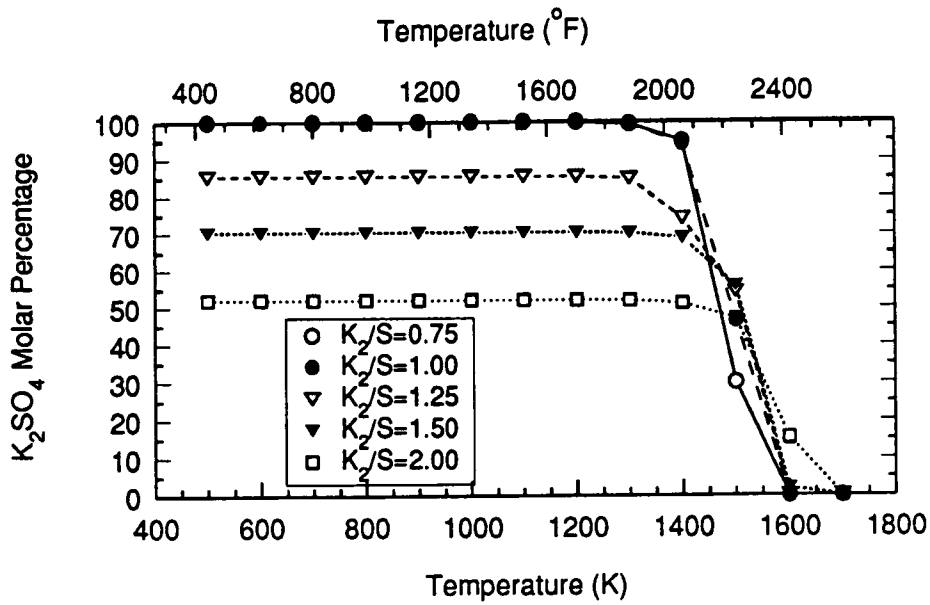


Figure 3-14. Fraction of Total Potassium Species as Condensed $K_2SO_4(c)$ vs. Temperature at Different K_2/S Ratios ($SR_1=0.85, SR_2=1.05$)

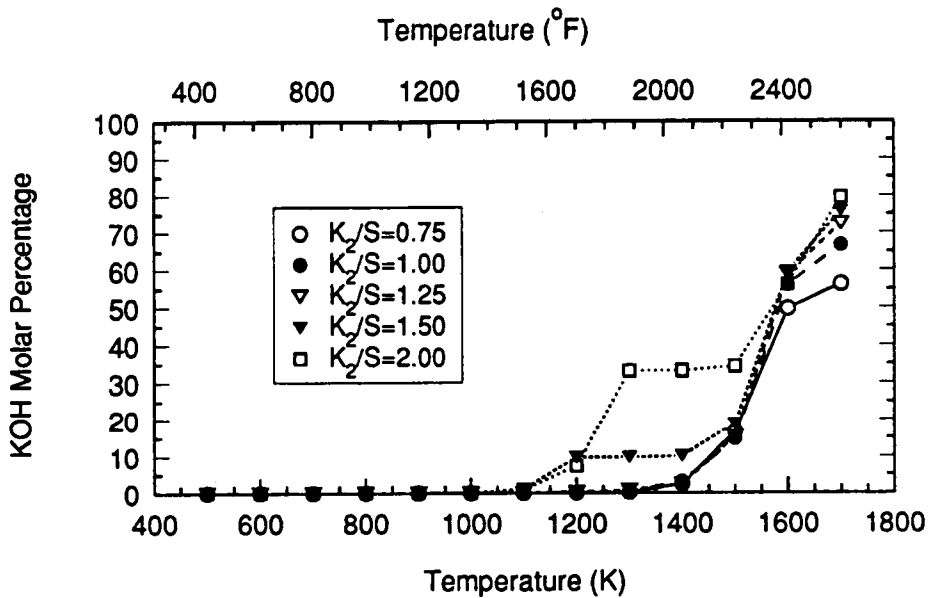


Figure 3-15. Fraction of Total Potassium Species as Gas Phase KOH vs. Temperature at Different K_2/S Ratios ($SR_1=0.85, SR_2=1.05$)

3.4.4. The Effect of SR2 on KOH and $K_2SO_4(c)$ after Secondary Combustion

Figures 3-16 and 3-17 show the effects of secondary stoichiometric ratio on the concentrations of $K_2SO_4(c)$ and KOH as molar percentage of the total potassium species for $K_2/S=1.25$.

Obviously, secondary stoichiometric ratio(SR2) as shown in Figures 3-16 and 3-17, has no effect on both the molar percentage of $K_2SO_4(c)$ and KOH.

3.5 Behavior of Minor Sulfur Species

As have been pointed out in section 3.4.1, some minor sulfur species, such as SO, S_2 , COS are also calculated to be formed along with the major sulfur species, i.e. SO_2 , H_2S before secondary combustion. Figures 3-18 to 3-21 show some of the most important characteristics of the behavior of minor sulfur species.

Figure 3-18 shows the relationship between molar percentage of selected sulfur species and gas temperature for $K_2/S=1.25$ and $SR1=0.85$. According to this figure, the molar percentage of SO decreases monotonically as temperature decreases. However, the molar percentages of SH, S_2 , and COS all have a maximum at a certain specific temperature. For example, SH molar percentage has its maximum of about 2 % at 1600 K; S_2 molar percentage has its maximum value of about 10 % at 1500 K; and COS molar percentage has its maximum of about 7 % at 1400 K. As can be seen, the total amount of these minor sulfur species can reach 20 % at certain temperatures.

Similar to the situation for SO_2 and H_2S , the K_2/S ratio has little effect on concentrations of these minor sulfur species. However, stoichiometric ratio can affect the concentration of these species as shown in Figures 3-19 to 3-21.

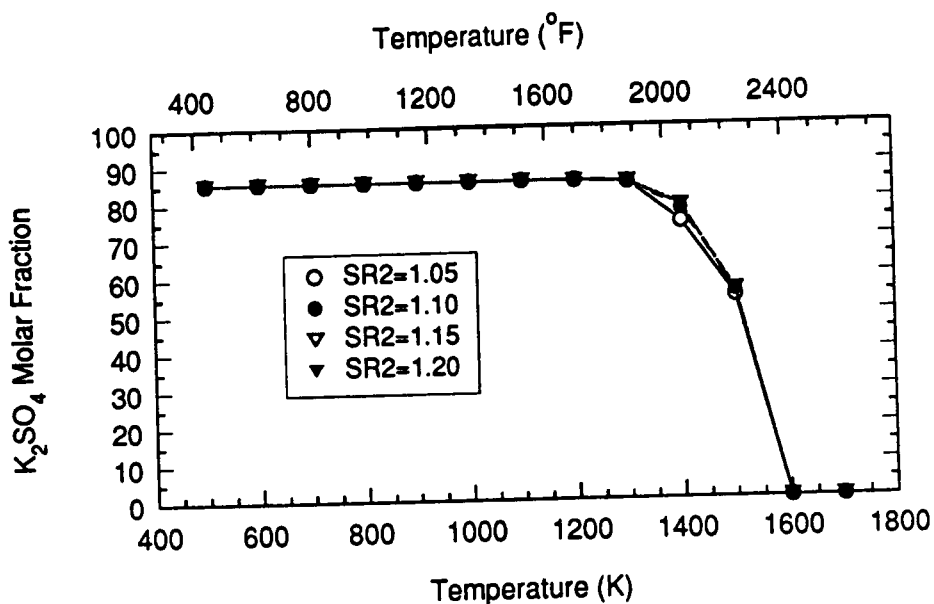


Figure 3-16. Fraction of Total Potassium Species as Condensed $K_2SO_4(c)$ vs. Temperature at Different $SR2(K_2/S=1.25, SR1=0.85)$

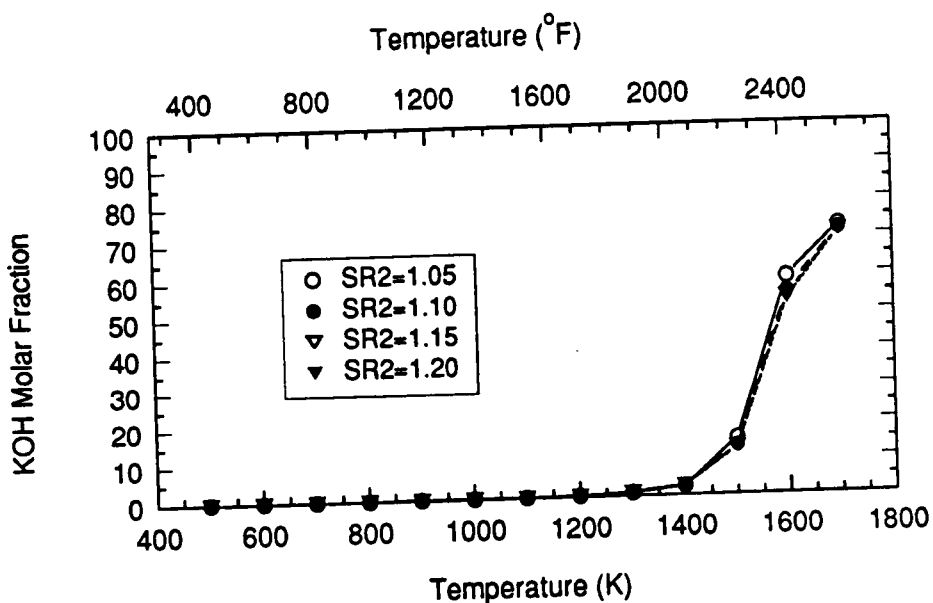


Figure 3-17. Fraction of Total Potassium Species as Gas Phase KOH vs. Temperature at Different $SR2(K_2/S=1.25, SR1=0.85)$

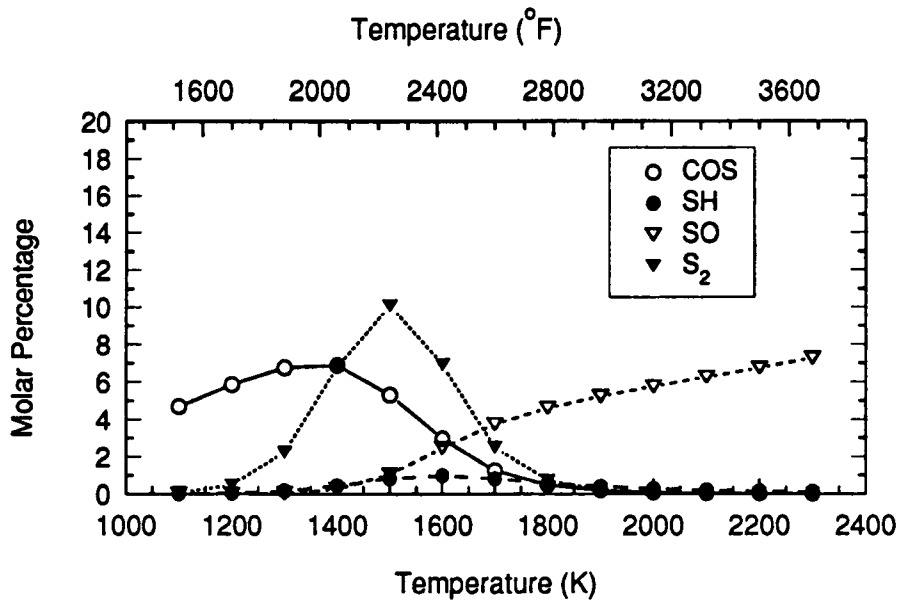


Figure 3-18. Fraction of Total Sulfur Species as Minor Sulfur Species vs. Temperature before Secondary Combustion ($K_2/S=1.25$, $SR1=0.85$)

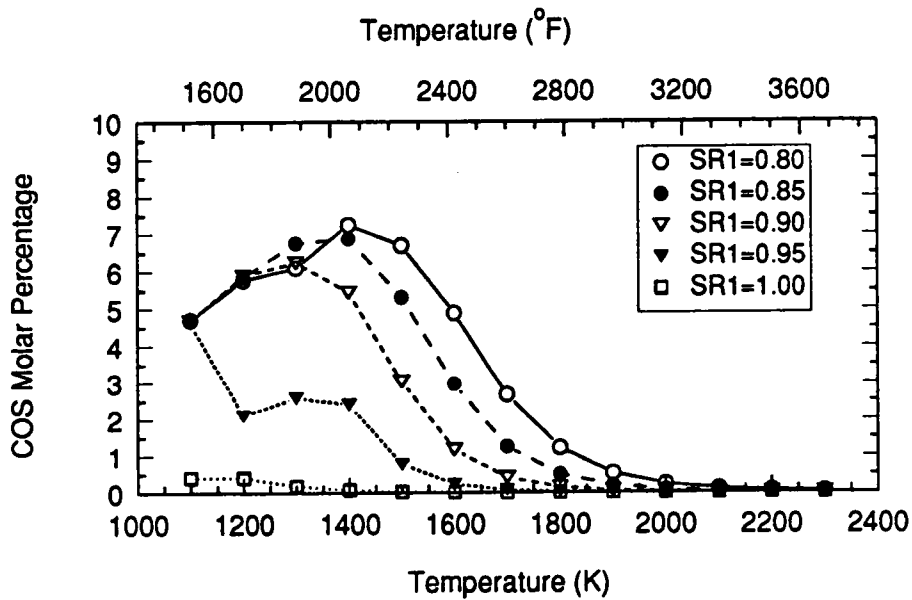


Figure 3-19. Fraction of Total Sulfur Species as COS vs. Temperature at Different SR1 ($K_2/S=1.25$)

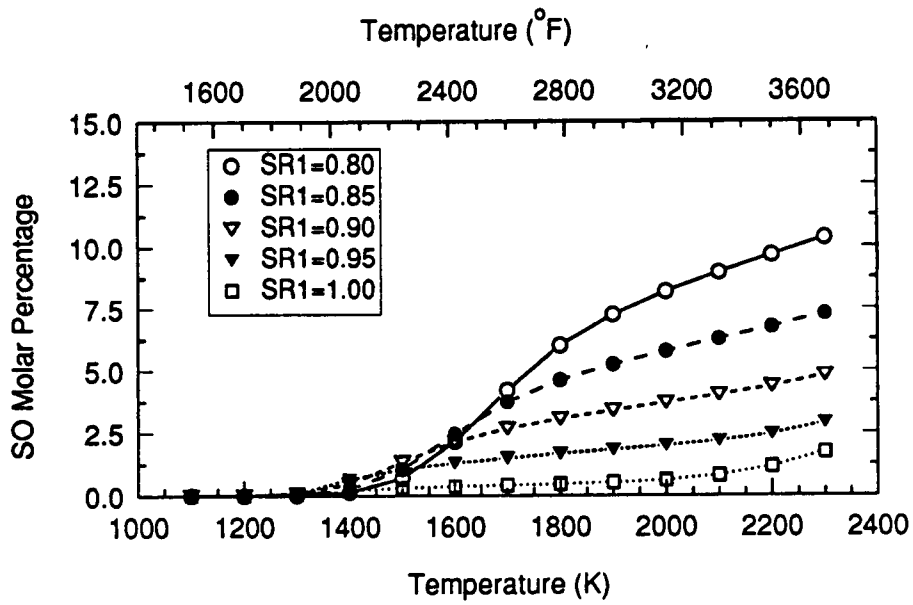


Figure 3-20. Fraction of Total Sulfur Species as SO vs. Temperature at Different SR1 ($K_2/S=1.25$)

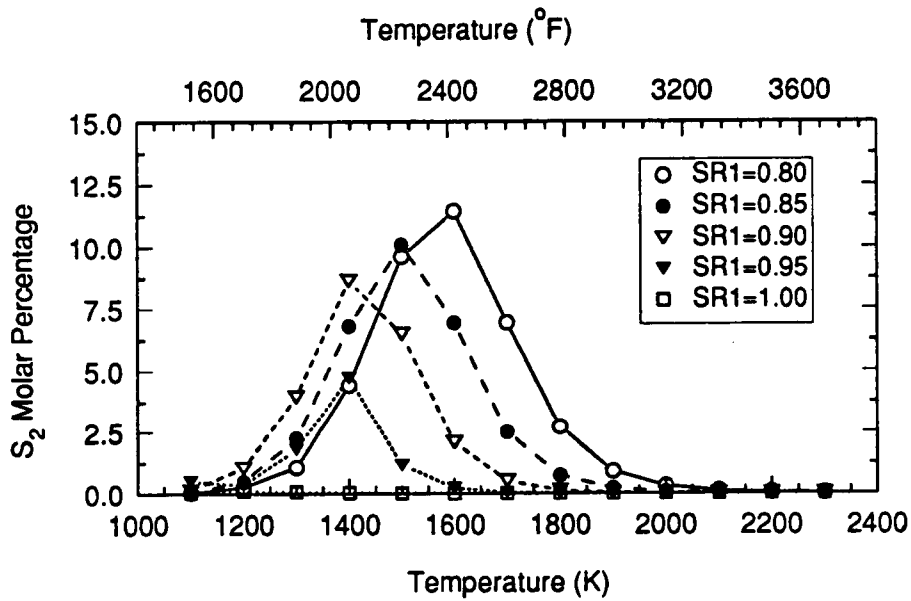
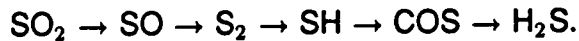


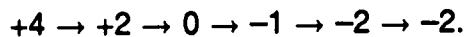
Figure 3-21. Fraction of Total Sulfur Species as S_2 vs. Temperature at Different SR1 ($K_2/S=1.25$)

It is expected that as the primary stoichiometric ratio increases, the concentration of sulfur species in reduced form will decrease, which is shown in Figure 3-19 and Figure 3-21. The molar percentages of S_2 and COS of the total sulfur species decrease as stoichiometric ratio increases. In contrary to expectation, the molar percentage of SO also decreases as stoichiometric ratio increases, according to Figure 3-20. This seems to happen because SO_2 has a greater affinity for O_2 than SO under this condition.

Looking into the transition of the valence of sulfur in these species is also interesting. As temperature decreases from 2300 to 1100 K, sulfur species has a transition from



Valence transition for these compounds follows as



These minor sulfur species, probably serve as a bridge, involved in the transition of sulfur species from SO_2 to H_2S before secondary combustion.

3.6 The Concentration of Gas Phase KS, K_2S , K_2SO_4 Species

It is possible now to assess the existence of gas phase KS, K_2S , K_2SO_4 species in view of their newly included thermodynamic data. Based on the calculations, the concentration of KS is very small in all cases. The concentration of K_2S , however, can not be neglected in some cases. There is a significant amount of gas phase K_2SO_4 after secondary combustion. Their dependence on gas phase temperature is shown in Figures 3-22 and 3-23.

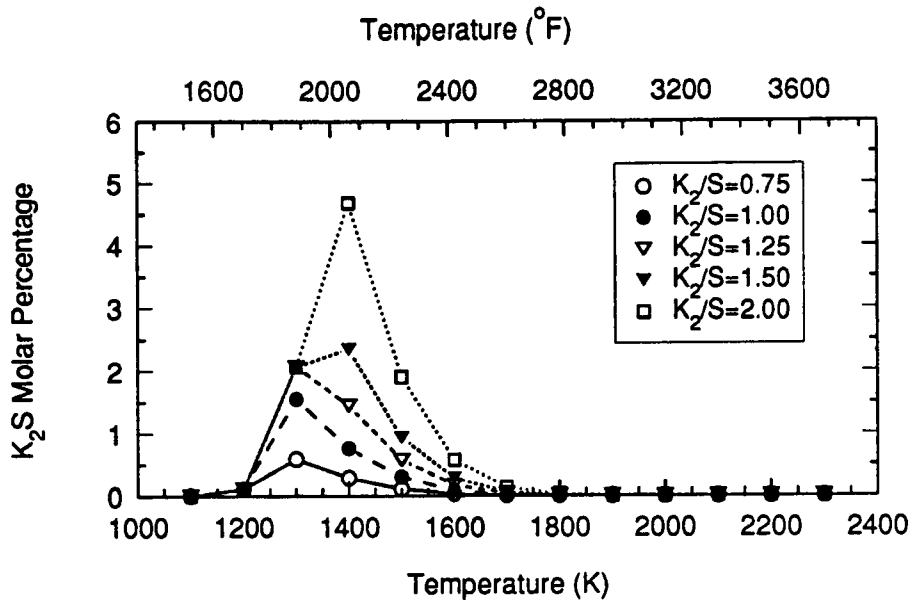


Figure 3-22. Fraction of Total Sulfur Species as Gas Phase K_2S vs. Temperature at Different K_2/S Ratios (SR1=0.85)

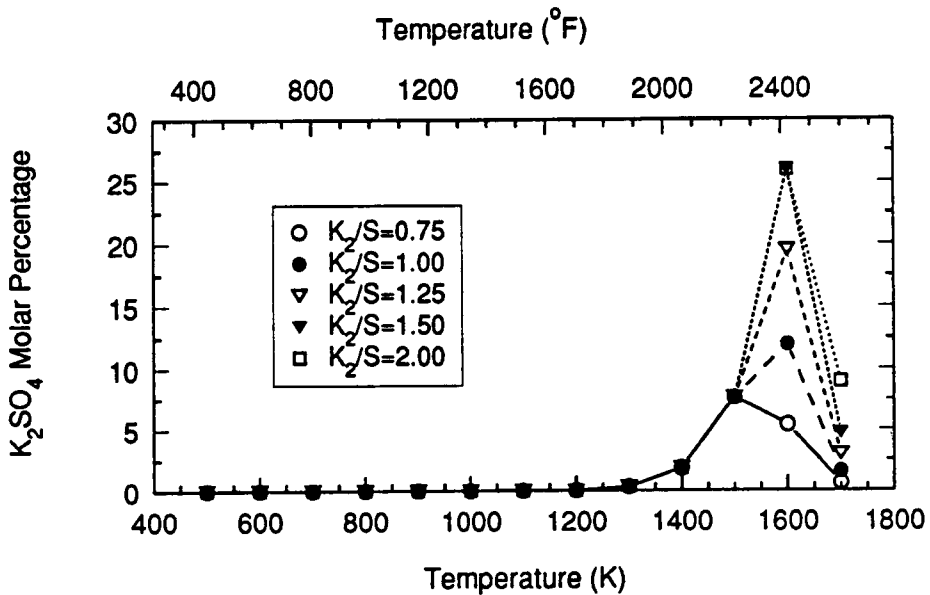


Figure 3-23. Fraction of Total Sulfur Species as Gas Phase K_2SO_4 vs. Temperature at Different K_2/S Ratios (SR1=0.85, SR2=1.05)

Figure 3-22 shows the relationship between molar percentage of the total sulfur species as K_2S and gas temperature at different K_2/S ratios. There is a maximum in the molar percentage of K_2S . It occurs at 1300 - 1400 K. At typical condition ($K_2/S=1.25$, $SR1=0.85$), molar percentage of K_2S is about 2 % of total sulfur species.

Figure 3-23 shows the relationship between molar percentage of the total sulfur species as K_2SO_4 and gas temperature after secondary combustion. There is also a maximum of molar percentage of K_2SO_4 . It occurs at 1500 - 1600 K. At typical condition ($K_2/S=1.25$, $SR1=0.85$, $SR2=1.05$), molar percentage of gas phase K_2SO_4 is about 20 % of the total sulfur species.

CHAPTER 4

COAL-FIRED FLOW FACILITY MEASUREMENTS

In order to determine the real concentration profiles in both gas and condensed phase species in the downstream of the CFFF, gas samples and aspirated particulate samples were collected during tests LMF4-U and LMF4-V. Three sampling locations were chosen, namely Radiant Furnace (RF1), Secondary Combustor Inlet (SCI), and Secondary Combustor Outlet (SCO). These sampling locations in the Coal-Fired Flow Facility are shown in Figure 4-1.

4.1 Sampling System

At the Coal-Fired Flow Facility, a gas phase sampling system has been established. This system has the capability to measure and analyze most of the major gas species, such as nitrogen, oxygen, carbon monoxide, carbon dioxide, SO_x, and NO_x, coming out of secondary combustor, BH/ESP, or stack. During the tests, the concentrations of these gas species are closely monitored. Based on these measured values, the performance parameters are adjusted to ensure operational satisfaction and environmental compliance.

More attention was paid to particulate sampling, because it is more difficult, more time consuming, and less developed. Figure 4-2 shows the sampling system used in the test LMF4-U. This test was conducted between August 1 to 13, 1990. This sampling system consists of a sampling probe, sampling box, primary filter, back filter, electric dryer, chiller, and an air eductor. When sampling, a mixture of gas and condensed species are aspirated from the combustion

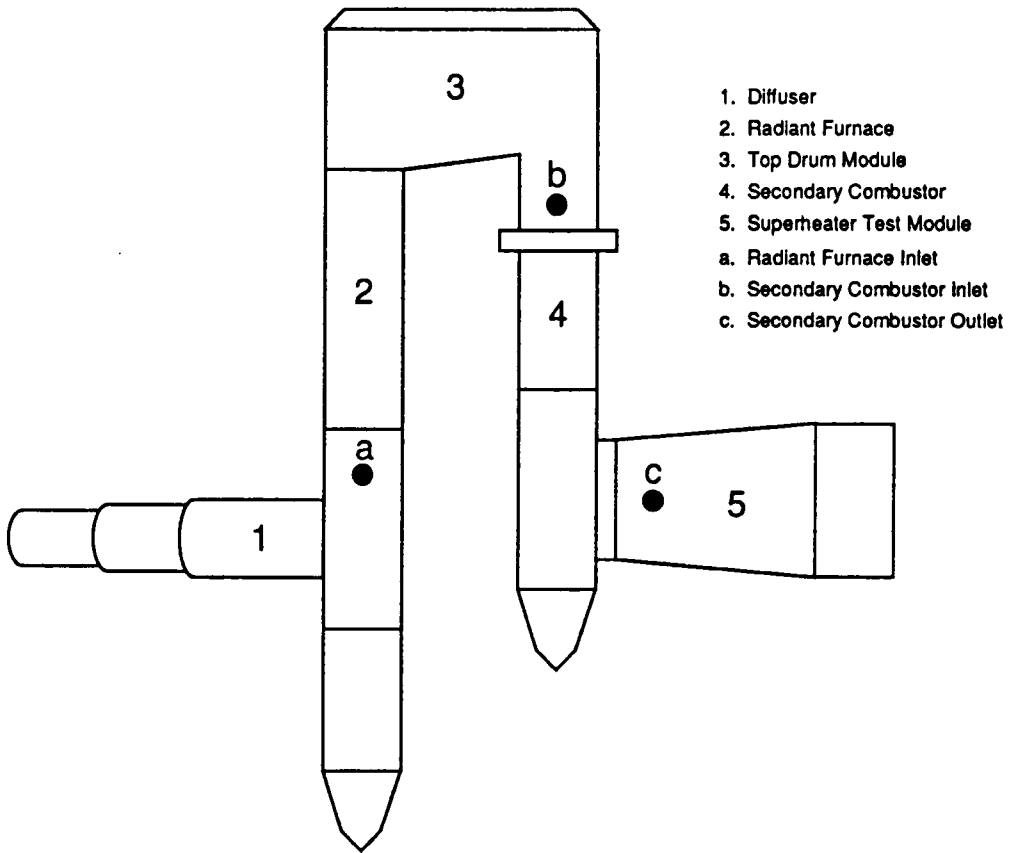


Figure 4-1. Sampling Locations in the CFFF

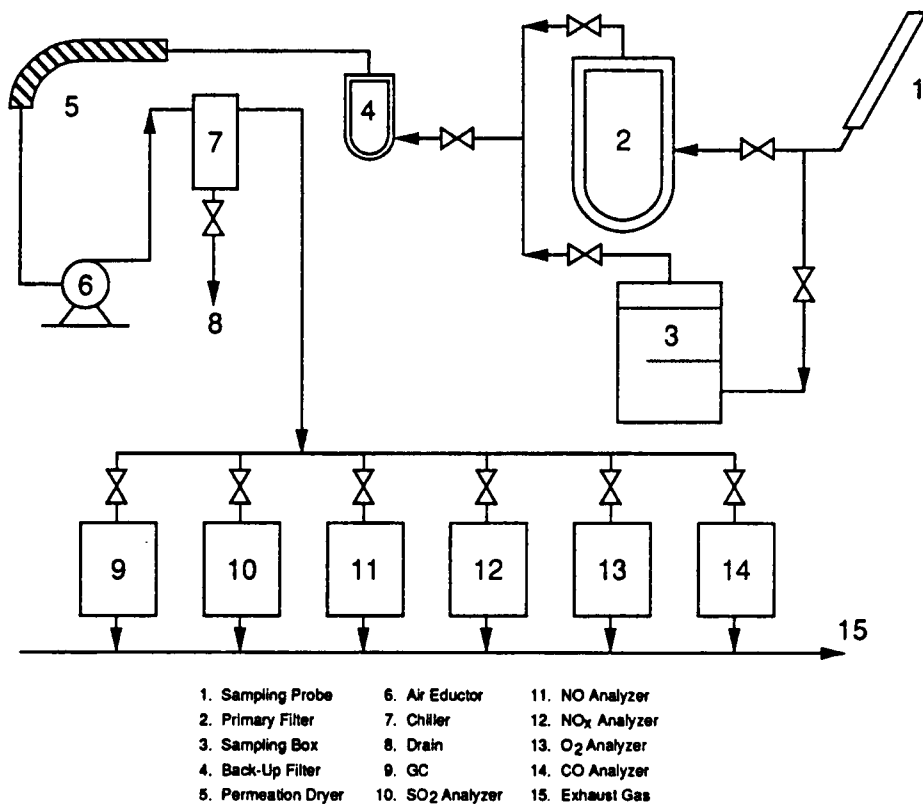


Figure 4-2. Aspirated Particulate and Gas Sampling System

system through a water cooled probe (1). The mixture then passes through either primary filter (2) (gas sampling only), or a sampling box (3) (gas and particulate sampling). The major part of the particulate in the mixture is blocked by the filter in the sampling box, and collected there. Remaining gas species with some very fine particulate entrained passes through a back filter (4). Primary filter (2), back filter (4), and sampling box (3) are maintained in a heated cabinet to prevent moisture condensation. After passing the back filter, all the particulates have been separated from gas species. The remaining gas phase species then pass through a dryer (5), are sucked in by an air eductor (6), then dried again by a chiller (7), and finally head for gas analyzer and/or gas chromatograph (GC) for analysis.

Figure 4-3 shows the sampling probe. It is a steel tube of approximately 6' in length, 4" in outer-diameter (OD) and 1.4" in inner-diameter (ID). Outside of the tube is surrounded by a water-cooled jacket. The cooling water is used to freeze the chemical reactions in the probe and to protect the probe from overheating. At the end of the probe, there is a watch-window covered by a plug. The sample path of the probe can be checked or unplugged through the window.

Figure 4-4 shows the sampling box. It is a 11.2" x 5.7" x 8.4" aluminum box. A gas exit tube is connected through the center of the cover. Under the cover, there is a rubber gasket, which provides the seal to the box. The box cover also has an attached spring. The spring supports a screen on the filter of the box when the box is closed.

The body of the box consists of two chambers divided by a partition. Filter cloth is placed on a protruding curb above the top chamber. A steel screen is put on top of the filter cloth in order to hold it. A mixture of gas and condensed phase species is pulled into the box from the gas flow inlet at the bottom.

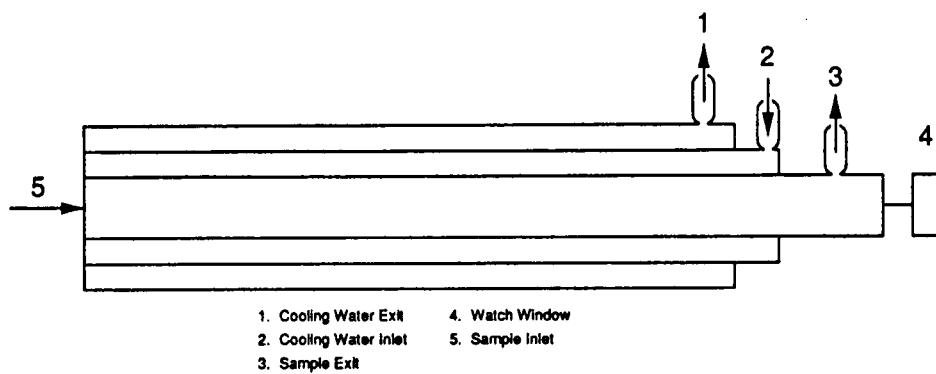
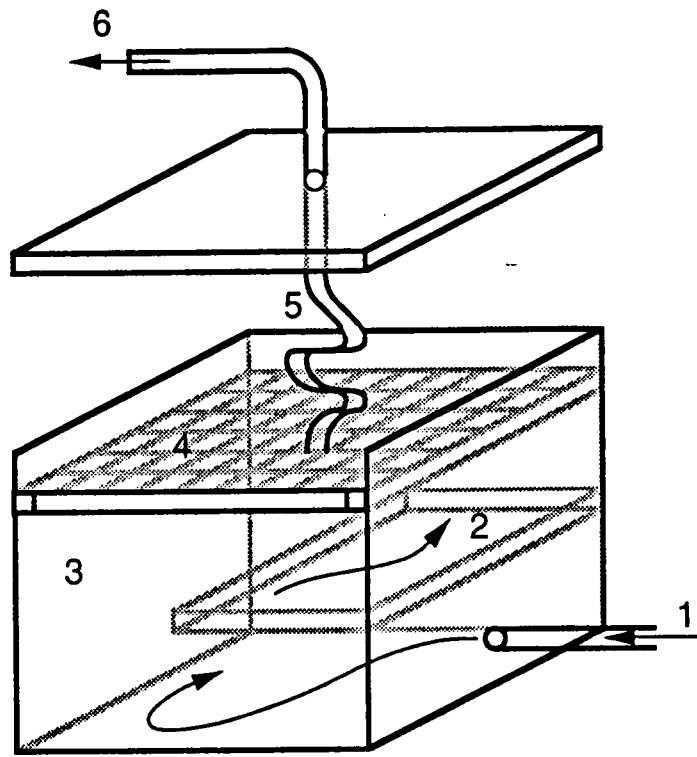


Figure 4-3. Sampling Probe



- | | |
|------------------------------|---------------|
| 1. Gas and Particulate Inlet | 4. Screen |
| 2. Partition | 5. Spring |
| 3. Filter Cloth | 6. Gas Outlet |

Figure 4-4. Sampling Box

Particulates are blocked by the filter cloth and collected in the two chambers of the box. After gas-solid separation, gas species go through the exit tube at the top, and to the gas analyzers.

4.2. Sampling Process

To collect particulate sample, the sampling box is cleaned and dried first. Then a new filter cloth is fixed carefully on the curb by the screen. The closed box is leak checked. This box is then installed inside the cabinet and connected to the sampling line. After preheating for about 40 minutes, the air eductor is turned on. Particulate sampling is then initiated.

Along with particulate sampling, gas sampling and analysis can be conducted simultaneously. The on-line gas chromatograph (GC) available in the gas analysis room is able to analyze major and trace species, such as H₂, O₂, N₂, CH₄, H₂S, CO, and NH₃. The gas analysis room is also equipped with two SO₂ analyzers, NO_x and NO analyzers, CO analyzers, and O₂ analyzers. Since there are only two SO₂ analyzers, sample lines have to be switched in order to analyze SO₂ from more than two locations.

The time needed to collect particulate samples varies at different locations. Among three locations where sampling was conducted, Secondary Combustor Outlet (SCO) is the easiest place to collect. It usually takes only 45 minutes to get sufficient sample (at least 10 grams). Secondary Combustor Inlet (SCI) is the most difficult place to collect. It takes at least four (4) hours to get a sample. The situation at Radiant Furnace (RF1) is only a little better than at SCI. It also needs more than four hours to collect enough for analysis.

A possible explanation to above phenomena can be that after secondary

combustion, most of the potassium would have reacted with the coal-bound sulfur forming significant amount of $K_2SO_4(c)$. Condensed $K_2SO_4(c)$ is easy to collect. However, at RF1 and SCI, not enough K_2SO_4 is expected to form. Other potassium compounds at these two locations have higher melting points (> 1000 K), and most likely would deposit in the relatively colder sampling probe and sampling line before they would arrive at the sampling box. Experiences gained from sampling support this hypothesis. The sampling probe and sampling line at RF1 and SCI were easily plugged by deposition. It was necessary to unplug the sampling probe and sampling line about every 30 minutes. Samples at RF1 are slightly easier to collect than at SCI. This is probably because of the slag existing in the radiant furnace. Part of the particulates collected at RF1 is assumed to be slag. While at SCI, the amount of slag is greatly reduced after the combustion products pass through the furnace and the top drum module.

After sampling for the suggested time, the sample boxes are purged with nitrogen. They are then taken off the sampling line and sent to the Chem Lab for analysis. Sampling boxes from the radiant furnace (RF1) and secondary combustor inlet (SCI) locations are opened in a transparent sealed bag purged with nitrogen. This is to prevent the particulate samples being oxidized by air. After the test, these samples are analyzed to determine potassium and sulfur levels and forms.

4.3. Data Analysis for Particulate and Gaseous Species

Samples collected at radiant furnace (RF1), secondary combustor inlet (SCI), and secondary combustor outlet (SCO) are analyzed at the Chem Lab of UTSI. The results of the analysis are presented in Table XI, XII and XIII.

Table XI. Particulate Analysis for Test LMF4-U

Location	Date	K%	S%			
			Total	Sulfate	Sulfide	Pyrite
SCO	08-02	38.96	13.5	13.6	0	NA*
SCO	08-04	40.41	14.3	13.9	0	NA
SCO	08-06	37.63	14.2	13.6	0	NA
SCO	08-07	39.81	14.6	14.1	0	NA
SCO	08-09	40.38	15.1	14.0	0	NA
SCO	08-10	38.64	NA	NA	NA	NA
SCO	08-11	39.06	NA	NA	NA	NA
RF1	08-04	NA	3.7	0.9	0.5	0.6
RF1	08-06	NA	5.8	1.1	0.4	2.1
RF1	08-10	35.48	3.3	0.7	0.2	NA
RF1	08-11	36.24	15.8	11.0**	NA	NA
RF1	08-13	32.78	NA	NA	NA	NA
SCI	08-10	33.10	4.2	1.1	0.1	NA
SCI	08-13	34.55	4.3	1.7	0.05	NA

*: Not Analyzed/Not Available

** : Inadvertently Oxidized

Table XII. SO₂ Measurements for Test LMF4-U

Location	Date	Time	SO ₂ (ppm)
RF1	08-06	1:40	30-40
SCI	08-06	2:00	28-35*
SCO	08-06	2:30	550-600**
RF1	08-07	3:40	25-35
SCI	08-07	2:50	17-22
SCO	08-07	2:20	470-600***

* stable at 32 ppm

** stable at 565 ppm

*** stable at 520 ppm

Table XIII. H₂S Measurements for Test LMF4-U

Location	Date	Time	H ₂ S (ppm)
RF1	08-09	3:40	2200
SCI	08-09	3:20	1540
SCO	08-09	2:30	180
RF1	08-11	2:20	2240
SCI	08-11	1:20	1530
SCO	08-11	5.30	230

It was found after the test that the on-line GC was not appropriately calibrated for H₂S analysis. Similar measurements were carried out in some early tests. The H₂S concentrations at SCO were found to be less than 10 ppm. Appendix B shows these results. Sulfur content was 2.5 % (wt) during those early tests.

In addition to the particulate and gaseous species collected at RF1, SCI, and SCO, gas samples were also collected from the stack. The analysis of samples collected at the stack can be used to assess the overall pollution control efficiency. The data of SO₂ emissions at stack are plotted in Figure 4-5. It is apparent from this Figure that the CFFF system has a great potential to control SO₂ emissions while firing high sulfur fuel.

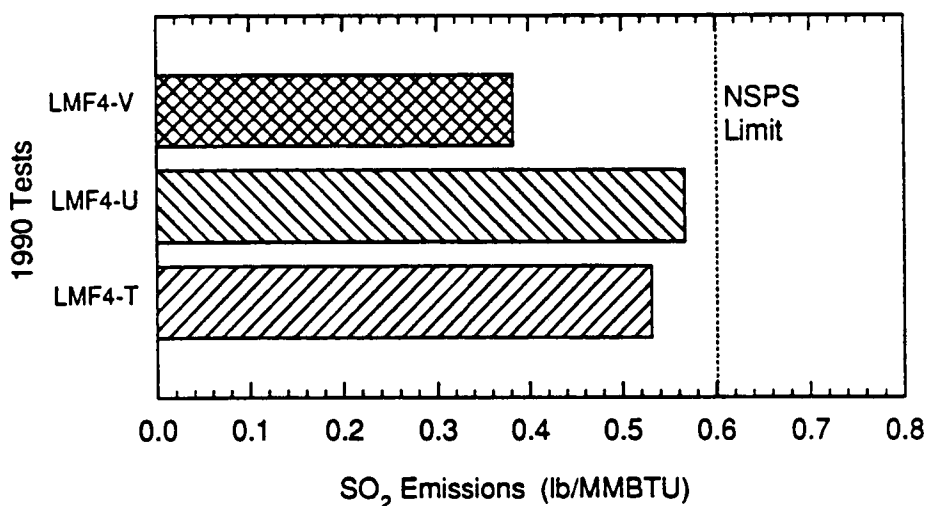


Figure 4-5. SO₂ Emissions at the Stack from CFFF

CHAPTER 5

COMPARISON OF RESULTS AND PROPOSED POTASSIUM-SULFUR REACTION STOICHIOMETRY

5.1 Comparison of Calculated Results with CFFF Measurements

In order to evaluate the validity of the equilibrium calculations, the results from calculations are to be compared with the CFFF measurements. Measured results have been presented in Chapter 4. Calculated results should be obtained from using the real operating conditions when the measurement is carried out. Most of the operating condition data can be obtained from an optical disk at UTSI, which records the operating parameters and on-line analysis data while the test is on. Table XIV through XVI list the operating parameters that are needed to carry out such calculations.

Based on these data, equilibrium calculations are carried out with modified NASA code, by which not only the molar fractions of species at equilibrium, but also the weight fractions of condensed species, real dry molar fractions of gas species (condensed species and H₂O excluded), the molar percentage of particular sulfur or potassium containing species over total sulfur species and/or over total potassium species, and total gas/total condensed phase ratio of sulfur or potassium species can be obtained.

Table XIV. Coal and Ash Analysis for Test LMF4-U

Proximate and Ultimate Analysis		Coal Ash Analysis	Wt %
Carbon (wt %)	66.60	SiO ₂	50.15
Hydrogen (wt %)	4.43	Al ₂ O ₃	67
Nitrogen (wt %)	1.67	Fe ₂ O ₃	12.85
Sulfur (wt %)	2.39	TiO ₂	1.03
Moisture (wt %)	3.30	CaO	3.27
Ash (wt %)	10.45	MgO	0.80
Heating Value	2.5660	Na ₂ O	0.51
(J/kg)	$\times 10^7$	K ₂ O	6.67
Chlorine (ppm)	2569	SO ₃	4.13

Source: Reported by Chem Lab at UTSI

Table XV. Fuel Oil Analysis for Test LMF4-U

Component	Wt (%)
Carbon	86.35
Hydrogen	13.54
Nitrogen	0.44
Sulfur	0.11
Heating Value	4.6120
J/kg	$\times 10^7$

Source: Reported by Chem Lab at UTSI

Table XVI. Major Operating Conditions for Test LMF4-U

Parameter	Value
Temperature at Primary Combustor(K)	3000
Temperature at RF1(K)	2300
Temperature at SCI(K)	1400-1450
Temperature at SCO(K)	1400-1550
Pressure at Primary Combustor(atm)	4.5
Pressure at Secondary Combustor(atm)	1.0
Coal Flow Rate(kg/sec)	0.32-0.41
Total Fuel Oil(kg/sec)	0.19
Oxygen (kg/sec)	0.84
Primary Air(kg/sec)	1.52
Upstream Purge N ₂ (kg/sec)	0.076
Downstream Purge N ₂ (kg/sec)	0.119
Secondary Air(kg/sec)	1.22
Primary Stoichiometric Ratio	0.80-0.88
Secondary Stoichiometric Ratio	1.05-1.10
K ₂ /S Ratio	1.0

Comparisons of calculated and measured results are presented in Table XVII and Table XVIII.

**Table XVII. Concentrations of Major Gas Phase
Sulfur Species for Test LMF4-U**

Location	Temperature (K)	Species	Measured* (ppm)	Calculated (ppm)
SCO	1450	SO ₂	500–600	600
SCI	1400	SO ₂	35	230
RF1	2300	SO ₂	40	2230
SCO	1450	H ₂ S	<10	0
SCI	1400	H ₂ S	1600	1810
RF1	2300	H ₂ S	2400	0

* Average data from Tables XII and XIII.

**Table XVIII. Concentrations of Condensed Phase Species
for Test LMF4-U**

Location	Temperature (K)	Species	Measured* wt (%)	Calculated wt (%)
SCO	1450	K	39.27	40.32
SCI	1400	K	33.83	38.93
RF1	2300	K	34.83	0.00
SCO	1450	S	13.84	14.45
SCI	1400	S	4.43	0.00
RF1	2300	S	4.25	0.00

* Average data from Table XI.

At secondary combustor outlet (SCO), according to Tables XVII and XVIII, measured and calculated values of SO_2 and H_2S concentration in the gas phase agree very well. The concentration of total potassium and total sulfur in the condensed phase also agree well. At secondary combustor inlet (SCI), measured and calculated values of concentration of SO_2 and H_2S in the gas phase also have a good agreement. With respect to condensed phase, the concentration of total potassium also shows a good agreement.

At radiant furnace (RF1), however, measured and calculated concentrations of gas phase species as well as those of condensed phase species do not agree. Besides, at secondary combustor inlet (SCI), some sulfur species in condensed phase (4.43 % by weight) were detected, while the calculation shows no condensed phase sulfur species should occur under this condition.

Qualitatively, at secondary combustor outlet and inlet, calculated values agree well with measured ones for both major gas phase species and condensed phase species of potassium and sulfur. At radiant furnace (RF1), calculated values show a big difference from measured ones.

The total sulfur elements measured in the condensed phase at SCI is possibly due to the condensation of $\text{S}_2(\text{g})$ and $\text{K}_2\text{S}(\text{g})$. Calculation shows that there are about 10 % S_2 and 2 % K_2S of the total sulfur species in the gas phase. In fact, the author did find some yellow crystals on the filter in the sample box located at SCI on August 7, 1990, which is suspected to be condensed S. This sample was insufficient to be analyzed at that time.

It is not surprising that the agreement between calculated and measured values is bad at the radiant furnace (RF1). The temperature is very high at that point. Chemical reactions and phase transition are very likely to take place in the sampling probe. Although heterogeneous reactions can not be modeled at

the present time, modeling of the gas phase reaction in sampling probe can be carried out using the PROF program. The following section describes the kinetic modeling of the potential gas phase reactions occurring in the sampling probe at radiant furnace (RF1).

5.2 PROF Code Modeling

The "Premixed One-dimensional Flame" computer program (PROF code) [4] can be used to predict the detailed chemical kinetic combustion and/or pollutant formation events for many combustion devices. Particularly, for a water-cooled sampling probe, the chemical kinetics in the probe can be modeled by the plug-flow reactor option of the PROF code. In this option, only radial diffusive heat and mass transfer are considered. The governing conservation equations can then be written as:

Species:

$$\dot{m} \frac{dY_i}{ds} = AW_i - C_w J_{w,i}$$

Energy:

$$\dot{m} \frac{dh}{ds} = AQ - C_w q_w$$

where

- | | |
|--|--------------------------------------|
| \dot{m} mass rate of gas, | Y_i mass fraction of species i , |
| s distance along flow axis, | A cross sectional area, |
| W_i chemical production rate of species i , | h enthalpy of bulk gas, |
| C_w circumference of bounding tube, | Q volumetric heat loss, |
| $J_{w,i}$ flux of species i at bounding tube wall, | |
| q_w heat transport at the bounding tube wall. | |

The initial conditions necessary to solve these differential equations are the initial

gas composition and temperature values. These equations are solved by simple space marching in the PROF code.

The inputs needed to run the PROF include initial concentrations of the reacting species, initial gas temperature, wall temperature, convective heat transfer coefficient of the probe, and a reaction set. The initial concentrations of the reacting species are calculated from the NASA code. Knisley [10] has proposed certain values for the heat transfer coefficient of the probe and wall temperature. Crawford [11] has collected a reaction set, which contains 112 different reactions that include 37 species of C, H, N, O, S elements.

The PROF code was run based on these information. The input file to the PROF code can be found in Appendix C. Table XIX shows the results from PROF calculation for the sampling probe at RF1 for test LMF4-U. These results reflect the concentration transformation of the gas species in the first 17.7 cm of the probe in 2.1 seconds. Meanwhile, gas temperature decreases from 2300 K to 1018 K. It should be noted that the heat transfer coefficient used was lower than that proposed by Knisley.

According to Table XIX, SO₂ concentration drops from 2231 ppm to 1260 ppm, while H₂S concentration rises from about zero to 959 ppm. Although the transformations of concentration do not match the CFFF measurements, this calculation does show the trend in SO₂/H₂S transformation and also indicates that there are significant chemical reactions taking place in the sampling probe. The slight disagreement of the calculated values from the PROF code and the measured values at CFFF may be because of insufficient kinetic data and inappropriate value of the heat transfer coefficient.

**Table XIX. Results from PROF Calculation for Test
LMF4-U at the RF1 Sampling Probe***

Species	Initial Concentration ×10 ⁶ ppm	Final Concentration ×10 ⁶ ppm	Rate of Change %
CO	0.11448E+00	0.99505E-01	-
CO2	0.18771E+00	0.20411E+00	-
H	0.13106E-02	0.89512E-08	-
H2	0.18618E-01	0.29602E-01	-
H2O	0.16829E+00	0.15799E+00	-
NO	0.54024E-03	0.13647E-03	-
N2	0.49831E+00	0.50105E+00	-
O	0.90039E-03	0.14958E-13	-
HO	0.18908E-02	0.10657E-09	-
O2	0.35015E-03	0.72714E-11	-
H3N	0.13229E-07	0.18146E-04	-
K	0.26412E-02	0.85744E-03	- 67.5
HKO	0.25111E-02	0.43312E-02	+ 72.5
KO	0.10004E-04	0.10657E-08	-
O2S	0.22310E-02	0.12605E-02	- 43.5
S	0.78864E-05	0.64088E-09	-
HS	0.41077E-05	0.68163E-06	-
S2	0.99963E-07	0.51793E-04	+ 51712
H2S	0.10957E-05	0.95893E-03	+ 87417
OS	0.19008E-03	0.17899E-05	- 99.1
O3S	0.27612E-06	0.15981E-07	-
COS	0.39558E-06	0.12200E-03	+ 30740

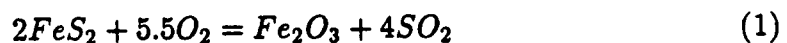
* Species with concentration less than 0.1 ppm are not included in the Table. These 15 species are: CN, CHN, HNO, HO2, N, NCO, HN, H2N, NO2, N2O, CHO, NS, CS, CS2, and OS2.

5.3 Proposed Potassium-Sulfur Reaction Stoichiometry

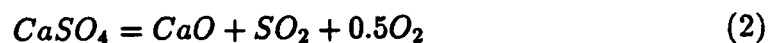
There are three competing chemistries with respect to potassium-sulfur reactions in CFFF: flame radical/sulfur chemistry, potassium oxidation chemistry, and potassium and sulfur reaction chemistry. Each of them is influenced by the others. As the reacting flow travels from primary combustor to secondary combustor and further downstream, gas phase temperature decreases from 2500 K to less than 1000 K. The operating condition also changes from reducing to oxidizing. Thus the dominating chemistry, if any, must change correspondingly. The following potassium-sulfur reaction stoichiometry is postulated based on previous researches and/or supported by the results of the above calculations and CFFF measurements.

5.3.1 Release of Coal-Bound Sulfur

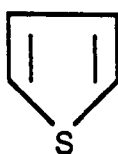
Two major inorganic sulfur forms in coal ash are pyritic sulfur (FeS_2) and sulfate sulfur (mainly as CaSO_4). At high temperature, the oxidation of pyrite to hematite (Fe_2O_3) occurs as follows [12]:



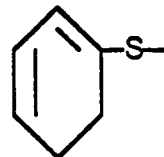
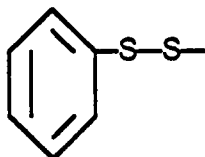
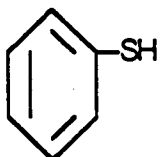
Sulfate sulfur will decompose at temperatures in primary combustor as follows [13]:



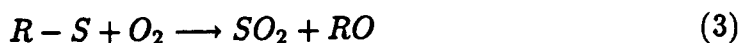
The dominant form of organic sulfur in the coal molecule is thiophene [14,15]. Solomon [16] indicates that as much as 60 % of the organic sulfur resides in such heterocyclic rings as:



Other organic sulfur forms listed by Wisler [14] are mercaptans, disulfides, and sulfides.

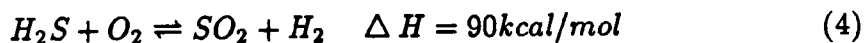


At temperatures above 1200 K [17], all these organic sulfur forms, including the stable thiophene, will decompose:



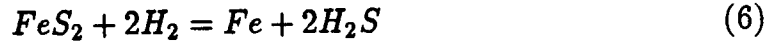
5.3.2. The Formation of Reduced Form of Sulfur Species

Our calculations show that SO_2 is the dominant sulfur species at temperature > 1600 K even under reducing condition. After temperature drops below 1600 K, H_2S becomes the dominant sulfur species. This may be due to the following reversible reaction [18]:



Higher temperature favors the forward reaction, while lower temperature favors the backward reaction.

The other reducing forms of sulfur species could be contributed by the following reactions:



As we also mentioned in Figure 3-2 and Figure 3-3, SO_2 concentration reaches a maximum before it decreases. While at the same time, SO concentration drops. This phenomenon can be explained by the following reaction:



5.3.3. Decomposition of Seed and Oxidation of Potassium

Seed ($K_2CO_3(s)$) added to the pulverized coal flow decomposes in the primary combustor via the following reaction:



Since the temperature is extremely high, part of the oxides may be further decomposed via the reaction



Other part of the potassium oxide may react with H_2O via the reaction

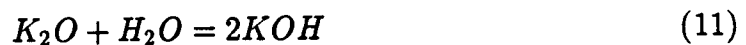
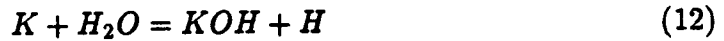


Figure 3-8 shows that at high temperature (2300 K), each of the molar percentage of K and KOH is about 50 % of the total potassium species.

As temperature decreases, the oxidation of potassium may continue via the reaction



The molar percentage of K decreases and that of KOH increases with decreasing temperature. When temperature is below about 1900 K, potassium silicate also occurs:



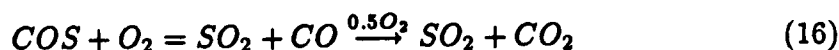
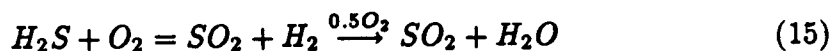
5.3.4 Dominant Chemistry before Secondary Combustion

By now it is clear that the dominant sulfur species are SO₂ and H₂S, and the dominant potassium species are K and KOH, before secondary combustion. No other potassium-sulfur compound or species are detected in significant amounts. Therefore it is believed that flame radical/sulfur chemistry and potassium oxidation chemistry probably dominate the chemical reactions occurring before the secondary combustion.

K₂S is also found before secondary combustion in equilibrium calculation. In fact, the K₂S concentration is about 2 % of the total sulfur species under typical condition, which is not very significant. Hence, it does not seem to change the overall course of potassium-sulfur chemistry.

5.3.5. Potassium-Sulfur Reaction Chemistry after Secondary Combustion

As preheated air is introduced into the secondary combustor, the reaction environment is converted from reducing to oxidizing. All the reduced forms of sulfur are thus oxidized:



Part of SO_2 may be further oxidized to SO_3 at certain conditions, especially at low temperature:

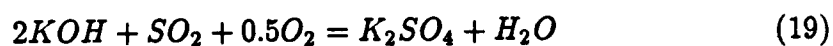


How sulfur (mainly as SO_2) reacts with potassium (mainly as KOH) to form potassium sulfate can be a controversial topic. Two options emerge: potassium sulfation occurs in the vapor phase and is followed by sulfate condensation; or occurs on ash and tube surfaces via a gas-liquid or gas-solid reaction mechanism. Calculations show that major part of potassium-sulfur reaction products is $K_2SO_4(c)$. This means that probably the major potassium-sulfur reaction occurs via:



In another words, potassium sulfation occurs via a heterogeneous gas/condensed phase reaction.

On the other hand, gas phase K_2SO_4 has also been found in equilibrium calculations. A typical value is 10 - 20 % K_2SO_4 of total potassium species, which is too big to be neglected. Thus it is reasonable to speculate that gas phase sulfation also occurs :



It should be noted that these conclusions are derived from the equilibrium calculations. However, chemical kinetics may play an important role. Similar research work on sodium-sulfur system did not exclude the possibility of vapor phase formation of Na_2SO_4 [19,20] either. Although, they predicted that there appears to be insufficient time for its formation in burnt combustion gases. Obviously, more work on the fundamental mechanism for potassium-sulfur reaction system is needed.

5.3.6. Overall Potassium-Sulfur Reaction Model

By now, we are able to summarize the stoichiometry of the possible potassium-sulfur interactions at different locations in the CFFF. Figure 5-1 is an overall model showing the possible potassium species, sulfur species and potassium-sulfur reaction compounds at different locations. This Figure also shows the major overall chemical reactions that lead to these species and compounds. At each location, namely RF1, SCI, SCO and BH/ESP, all the equilibrium species are listed in a box. These boxes are usually divided into three parts, listing the sulfur species, potassium species, and potassium-sulfur, potassium-slag, or potassium-carbon reaction compounds, respectively.

From Primary Combustor to Radiant Furnace, part of the potassium seed will react with the slag, and be rejected at Radiant Furnace. Equilibrium calculations do not show the existence of potassium-slag species, because the temperature is very high, and the thermodynamic data for these possible species in gas phase are not available. Thus, in the box for RF, gas phase K_2SiO_3 is followed by a question mark. Major sulfur species at RF is SO_2 , with the rest of the sulfur species as H_2S , S_2 , COS , SO , etc. Major potassium species at RF are K and KOH and they are in about the same amounts.

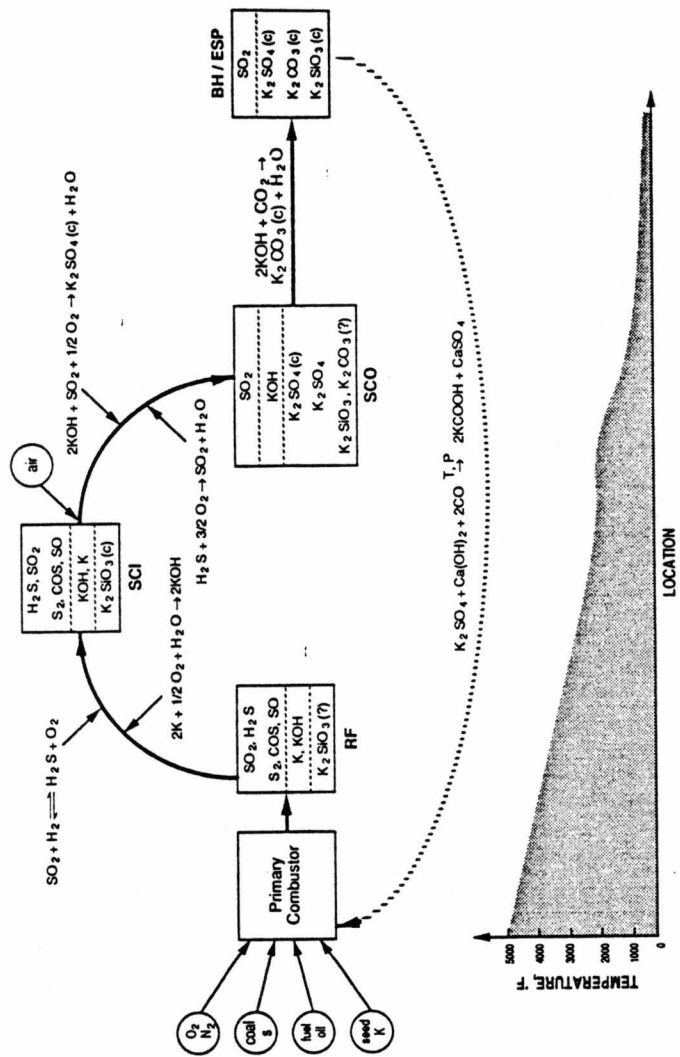
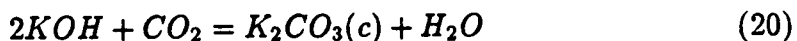


Figure 5-1. Overall Potassium-Sulfur Interactions Model at the CFFF

At SCI, the major sulfur species is H₂S, with the rest of the sulfur species as SO₂, S₂, COS, SO, etc. Major potassium species are KOH and K. The amount of KOH is greater than that of K. At relatively low temperature, K₂SiO₃(c), which should be interpreted as potassium-slag reaction species, may exist. The major chemical reactions taking place from RF to SCI are reactions (4) and (11).

At SCO, the operating condition has been changed from reducing to oxidizing with the introduction of excess secondary air. Most of the sulfur species have reacted with potassium species to form K₂SO₄(l,s). Other sulfur species (mainly as SO₂) are in a very small amount. Excess potassium species (mainly as KOH) is supposed to react with CO₂ to form potassium carbonate. But again the thermodynamic data for gas phase K₂CO₃ is not included in the data base of the NASA code. Thus K₂CO₃ is also followed by a question mark. The major reaction in secondary combustor is reaction (18).

From Secondary Combustor Outlet (SCO) down to BH/ESP, SO₂ concentration becomes lower and lower. So does the KOH concentration. However, condensed phase K₂CO₃(c) attains its equilibrium concentration at about 1100 K (from Fig. 3-7). Probably, excess KOH will react with CO₂ in the Superheater as



Spent seed (K₂SO₄(s)) collected at BH/ESP could be regenerated by either of the two similar seed regeneration processes – Formate Process and Econoseed Process. The overall chemical reaction is



If necessary, potassium formate could be oxidized further to potassium car-

bonate:



5.4 Empirical Equations for SO₂ Concentration after Secondary Combustion

5.4.1 Parameters Influencing SO₂ Concentration

SO₂ is usually the major sulfurous pollutant emission from coal-fired combustion processes. An empirical equation, which correlates the SO₂ concentration with all the major influencing parameters, is desirable. If we can find such an equation applicable to our CFFF system, minimizing the SO₂ emission could become a much easier task.

In section 3.3, the effects of temperature, K₂/S ratio, and secondary stoichiometric ratio on the SO₂ concentration have been investigated. Another possible influencing parameter that has not yet been discussed is the primary stoichiometric ratio. Figure 5-2 shows the relationship between the molar fraction (ppm) of SO₂ and temperature at different primary stoichiometric ratios with K₂/S=1.25 and SR2=1.05.

From Figure 5-2, we see that SR1 does not affect the SO₂ concentration after secondary combustion, provided that the SR2 is fixed. It should be noted that temperature above 1600 K is a hypothetical situation. Secondary combustion at the CFFF is never carried out above 1600 K.

We can now limit the major influencing parameters on SO₂ concentration as the gas temperature (T), potassium-to-sulfur ratio (K₂/S), and secondary stoichiometric ratio (SR2).

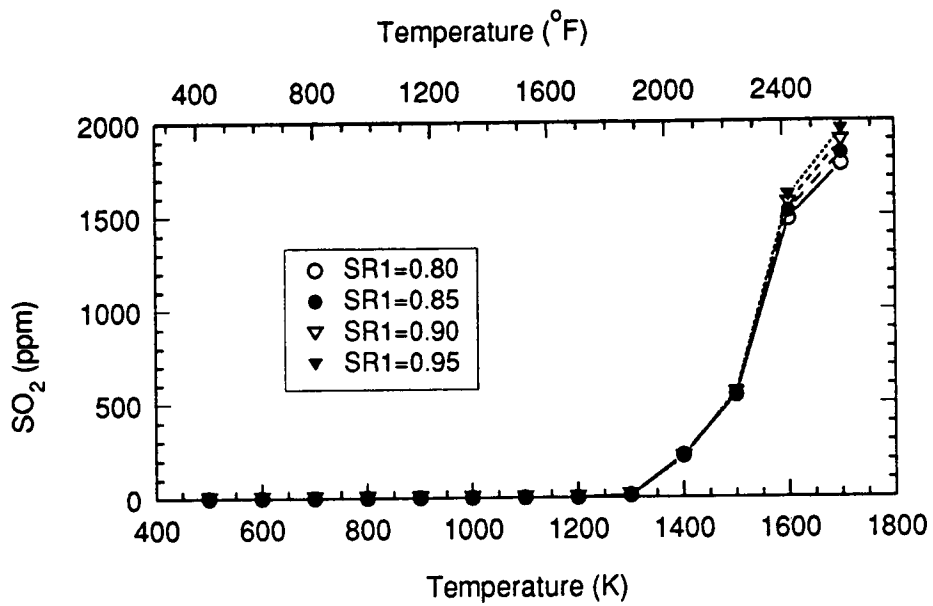


Figure 5-2. SO₂ Concentrations (wet basis) after Secondary Combustion vs. Temperature at Different SR1 ($K_2/S=1.25, SR2=1.05$)

5.4.2 An Empirical Equation for SO₂ Concentration

To determine an empirical equation in a proper form, we can start with the figures that reflect the relationship between SO₂ concentration and gas temperature, K₂/S ratio, and SR2. Figures 5-3 – 5-6 have shown these relationships.

From Figures 5-3 and 5-4, we can guess that SO₂ concentration is roughly related to gas temperature exponentially. From Figure 5-5, we can also guess that SO₂ concentration bears probably a reciprocal type relation with the K₂/S ratio. From Figure 5-6, we know that SO₂ concentration is a weak function of SR2.

On the other hand, we can start with the major chemical reaction:



At equilibrium, we have

$$\Delta G^\circ = -RT \ln K_p \quad (5.1)$$

where ΔG° is the standard molar Gibbs function for the reaction. R the gas constant, T the reaction temperature (K), K_p the equilibrium constant.

$$K_p = \frac{[K_2SO_4][H_2O]}{[KOH]^2[O_2]^{\frac{1}{2}}[SO_2]} \quad (5.2)$$

where $[K_2SO_4]$, $[H_2O]$, $[KOH]$, $[O_2]$, $[SO_2]$ represent the partial pressure of the species. Substituting equation (5.2) into (5.1), we have

$$\Delta G^\circ = -RT \ln \frac{[K_2SO_4][H_2O]}{[KOH]^2[O_2]^{\frac{1}{2}}[SO_2]}$$

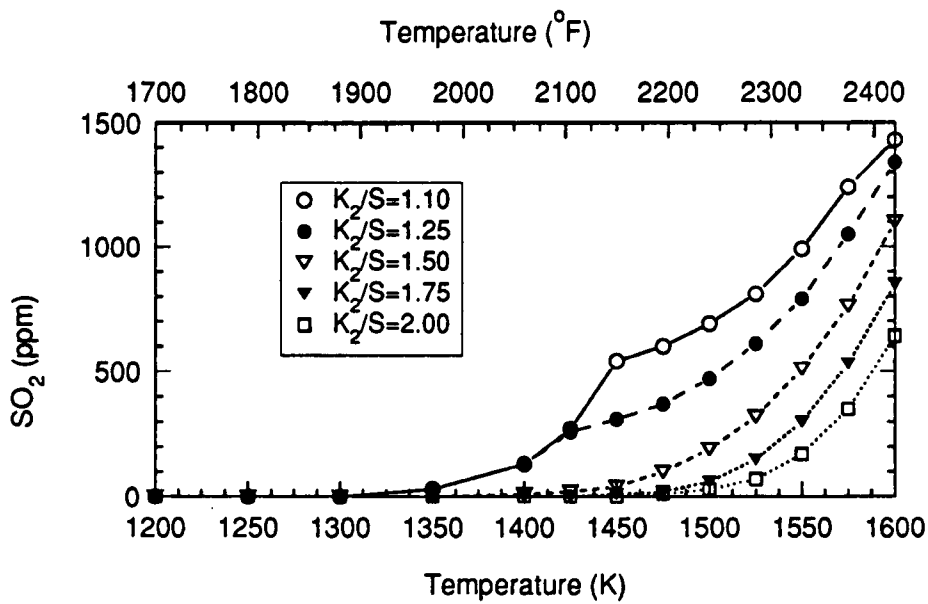


Figure 5-3. SO₂ Concentrations (wet basis) after Secondary Combustion vs. Temperature at Different K₂/S Ratios (SR1=0.85, SR2=1.10)

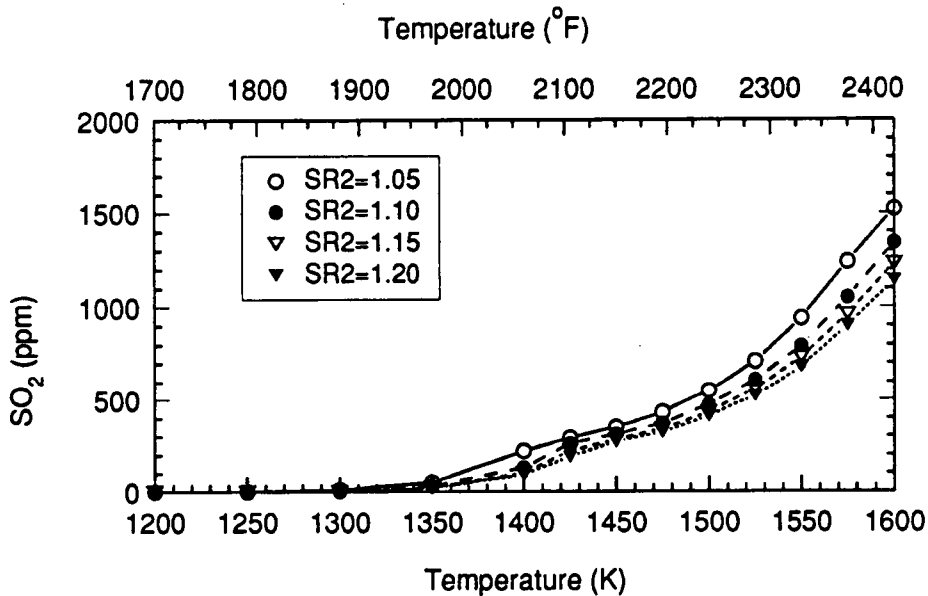


Figure 5-4. SO₂ Concentrations (wet basis) after Secondary Combustion vs. Temperature at Different SR₂ (K₂/S=1.25, SR1=0.85)

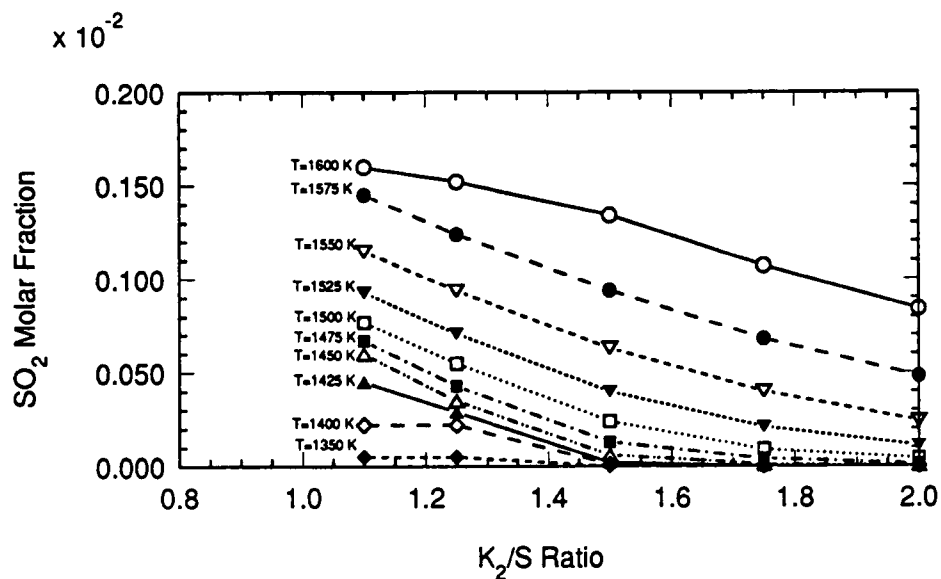


Figure 5-5. SO₂ Concentration (wet basis) after Secondary Combustion vs. K₂/S Ratio at Different Temperatures (SR1=0.85, SR2=1.05)

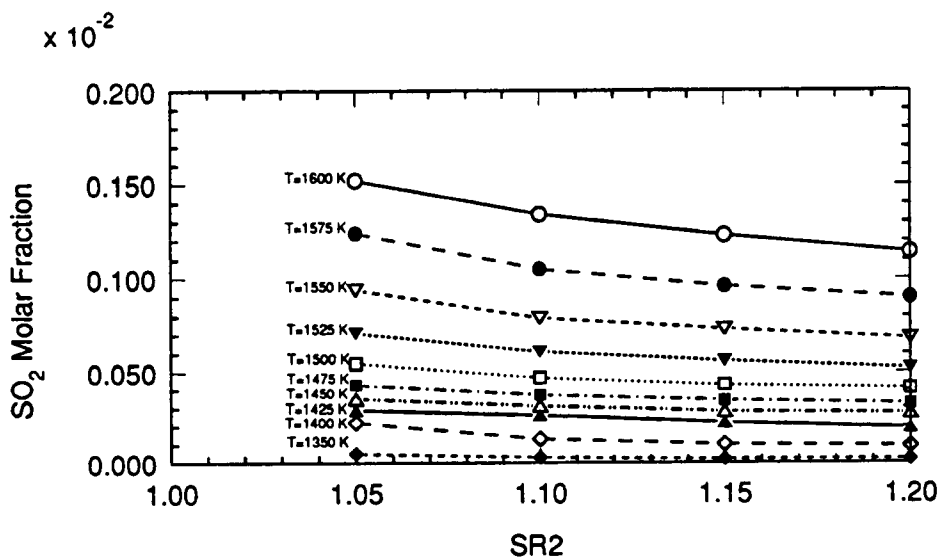


Figure 5-6. SO₂ Concentration (wet basis) after Secondary Combustion vs. SR2 at Different Temperatures (K₂/S=1.25, SR1=0.85)

or

$$[SO_2] = \frac{[K_2SO_4][H_2O]}{[KOH]^2[O_2]^{\frac{1}{2}}} e^{\frac{\Delta G^\circ}{RT}} \quad (5.3)$$

From above analyses, we assume that SO_2 concentration (ppm) can be expressed as

$$[SO_2] = \frac{A}{\gamma\theta^{\frac{1}{2}}} e^{-\frac{B}{T-C}} \quad (5.4)$$

where

- $[SO_2]$: SO_2 concentration in ppm
- T : gas temperature K
- A, B, C : functions of K_2/S ratio and SR2
- γ : potassium-to-sulfur ratio(K_2/S)
- θ : secondary(overall) stoichiometric ratio(SR2)

C is actually the temperature where SO_2 concentration approaches zero. From Figures 3-7, 5-3 and 5-4, we know that C is only a function of K_2/S ratio, and

$$C = 1000 + 200\gamma \quad (5.5)$$

The SigmaPlot program [21] was used to find the coefficient of A and B . The final equations obtained are

$$A = 33252.9\gamma + 13604.2\theta - 15088.4\gamma\theta - 19120.9 \quad (5.6)$$

$$B = -125.6\gamma + 417.4\theta + 488.5 \quad (5.7)$$

It should be noted that equations (5.4 – 5.7) are derived when $\gamma \geq 1.1$ and $\theta > 1.0$. Therefore, these equations can be used only under the similar conditions.

The comparison of results from the mathematical equations and from equilibrium calculations is shown in Figure 5-7. From this Figure, we see that equations (5.4 – 5.7) fit the equilibrium calculations well.

The fit of the derived equations with the CFFF measurements has also been checked. The result is presented in Figure 5-8. This Figure shows that the most of the measurement data from recent tests can be satisfied by these equations. The measurement data are within 20 % error bands from the values estimated by equations (5.4 – 5.7).

5.4.3 Sensitivity Analysis

We have obtained the empirical equation that correlates all the major influencing parameters on the SO₂ concentration. It will be useful to clarify the contributions of each parameter to the SO₂ concentration. Figures 5-9 and 5-10 are used to show the sensitivity of SO₂ concentration to K₂/S ratio and SR₂.

The sensitivity of SO₂ concentration to the gas temperature is shown in Table XX.

**Table XX. Sensitivity of SO₂ Concentration
to Gas Temperature at SR₂=1.10**

Temperature(K)	SO ₂ concentration(ppm)	
	K ₂ /S=1.10	K ₂ /S=1.25
1400	137	137
1450	364	245
1500	682	537

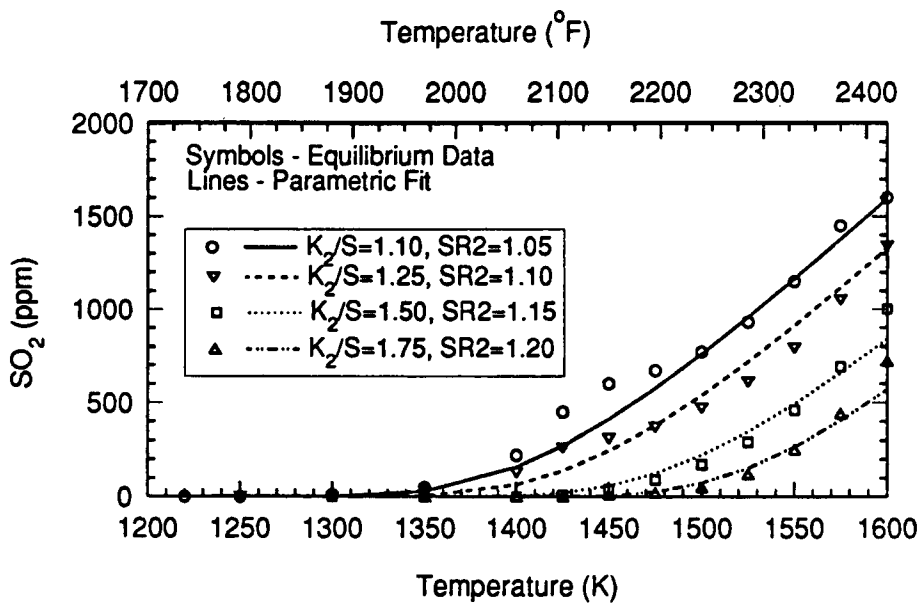


Figure 5-7. Comparison of Model Predictions with Equilibrium Calculations

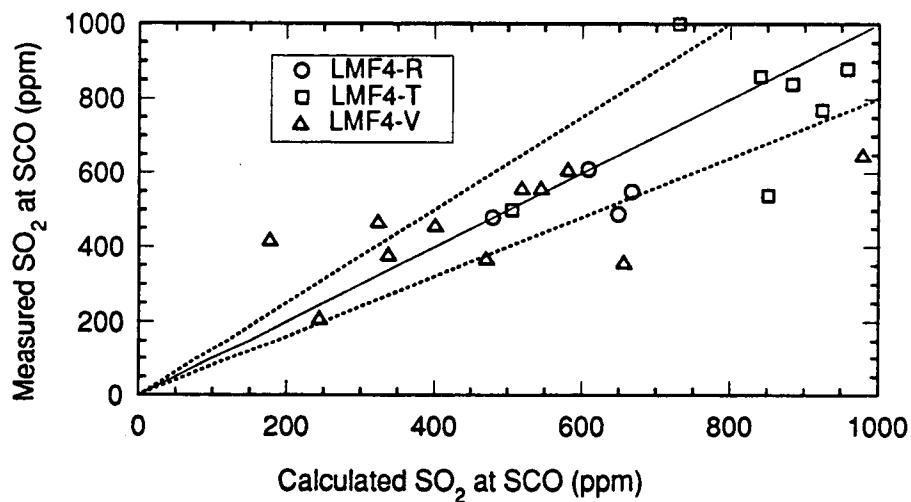


Figure 5-8. Comparison of Model Predictions with CFFF Measurements

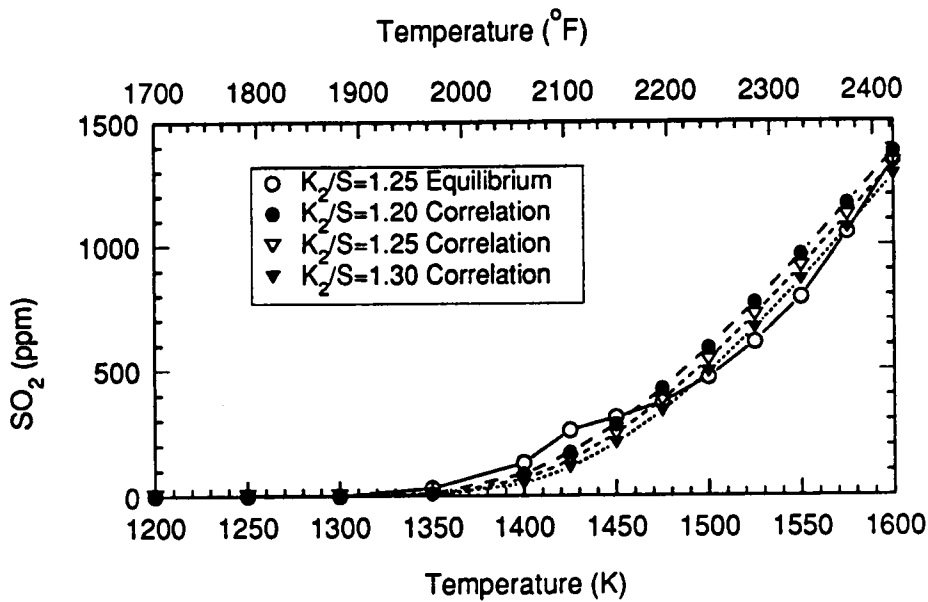


Figure 5-9. Sensitivity of SO_2 Concentration with respect to K_2/S Ratio ($\text{SR1}=0.85, \text{SR2}=1.10$)

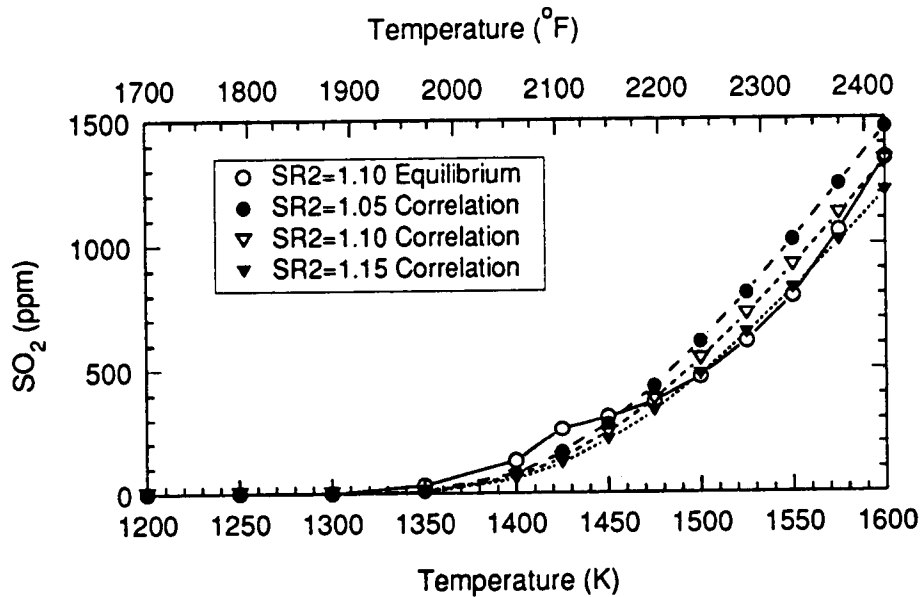


Figure 5-10. Sensitivity of SO_2 Concentration with respect to SR2 ($K_2/S=1.25, \text{SR1}=0.85$)

From the above Figures and Table, we can conclude that the gas temperature is the most sensitive parameter affecting the SO_2 concentration, followed by potassium-to-sulfur (K_2/S) ratio. Among the three major parameters, secondary stoichiometric ratio (SR2) is the weakest parameter affecting the SO_2 concentration.

5.5 Error Sources

In the course of potassium-sulfur reaction modeling, errors could be introduced in different forms. In this section, some major potential error sources are discussed.

(1) Physical Model Error: As has been mentioned several times, the NASA code is used to calculate the concentration of species presented and their distributions at equilibrium. In an MHD system, the combustion reactions take place very quickly. We can assume that the equilibrium condition is attained. The NASA code can be used to model the chemical reactions in the MHD system. However, as temperature decreases, especially after secondary combustion, chemical kinetics will play a more and more important role. Hence the assumption of equilibrium condition may be inaccurate at that location.

The program also assumes that the ideal gas behavior is followed, even when up to several percent by weight of condensed species are present. However, this assumption may cause errors when modeling the heterogeneous reactions taking place after secondary combustion.

(2). Sampling Error: A sampling system has to maintain the conditions of the sampling point. At the CFFF, however, the concentrations of gas and condensed species can not be measured instantly. Therefore, sampling errors are

inevitably introduced. At high temperatures, chemical reactions may take place in the sampling probe or sampling line. This has already been shown by the PROF calculation. Besides, sampling probes at Radiant Furnace and Secondary Combustor Inlet are easily plugged. Unplugging the probes may cause air leaks, which could affect the reducing condition required at these two locations.

(3). Measurement Error: Temperature measurement is the most difficult task. At such high temperatures (above 1400 K), a difference of 100 K in reading is likely to happen. This will affect the results of modeling the most. Other measurements can also introduce some errors in the modeling calculations. For example, measured primary and secondary stoichiometric ratios may be different from the actual values because of the air leak in the system. Therefore, the calculations could be affected by such inaccurate measurements.

These errors, along with some analytical errors, all can affect the accuracy of the reaction modeling in one way or another. However, one should not stop the modeling efforts, as it is very important for understanding the potassium - sulfur reaction processes. Nor can one diminish the importance of the model, as all such errors can be within the limitations (less than 20 %) accepted for an engineering design/estimate.

CHAPTER 6

CONCLUSIONS AND RECOMMENDATIONS

6.1 Conclusions

From the equilibrium calculations and CFFF measurements presented in previous chapters, the following conclusions can be drawn:

- flame radical/sulfur chemistry and potassium oxidation chemistry dominate the chemical reactions before secondary combustion, while potassium-sulfur reaction chemistry dominates the chemical reactions after secondary combustion.
- An empirical equation for SO_2 concentration after secondary combustion is derived. The agreement between the equation estimate and the equilibrium calculation is very good. Most of the CFFF measurements after secondary combustion could be well predicted by this equation as well.
- Results of calculations and measurements agree well for potassium and sulfur species both in gas and condensed phases at SCI and SCO locations. These results do not agree well at RF1 because of probable cooling effects in the sampling probe.
- With newly included thermodynamic data, about 10 - 20 % of total potassium species is detected as gas phase K_2SO_4 after secondary combustion. Therefore, $\text{K}_2\text{SO}_4(\text{c})$ is also believed to form through gas phase homogeneous reaction besides normally conceived heterogeneous reactions.
- Measured as well as calculated emissions of SO_2 are well below the current New Source Performance Standard(NSPS) limits at the CFFF operating conditions.

- The effects of CFFF operating parameters on the concentrations of various potassium and sulfur species are summarized in Table XXI.

Table XXI. The Effects of Operating Parameters on Major Species

Species	Before Secondary Combustion			After Secondary Combustion			
	T (K)	K ₂ /S	SR1	T (K)	K ₂ /S	SR1	SR2
SO ₂	***	o	**	***	**	o	*
H ₂ S	***	o	**	-	-	-	-
K	**	*	*	-	-	-	-
KOH	***	*	**	*	*	o	o
K ₂ SO ₄	-	-	-	*	*	o	o
K ₂ SO ₄ (c)	-	-	-	*	**	o	o
K ₂ CO ₃ (c)	-	-	-	**	*	o	o

*** strongly affected; ** affected; * slightly affected;
 o not-affected; - does not exist

6.2 Recommendations

Through the studies carried out in this thesis, a preliminary reaction model of potassium-sulfur interaction across the secondary combustor has been established. However, there is a lot to be done in this area. Some of the suggestions for future work are as follows:

(1) The empirical equation needs to be implemented to satisfy the SO₂ measurement data further downstream from the secondary combustor outlet. Since several hundreds ppm SO₂ is usually measured at the stack location, there should be a temperature at which SO₂ reaction/conversion is switched from thermodynamically to kinetically. This temperature is very likely in the region of

900 - 1200 K, or the superheater temperature range.

(2) Gas temperature should be measured more accurately. As described above, SO_2 concentration is very sensitive to the gas temperature.

(3) More condensed phase samples should be collected. Improving the sampling system would be a plus. With more particulate samples and their analysis results, condensation phenomena and cooling effects in sampling probe can possibly be investigated.

(4) Intermediate sulfur species should be measured. As shown by the calculations, several intermediate sulfur species, such as S_2 , COS , SO , may exist in the system. Their concentrations need to be measured to fully understand the sulfur chemistry during this two stage combustion process.

(5) Interactions of sulfur species with other species should be investigated. In coal-fired MHD system, there are a lot of gaseous and condensed phase species besides potassium and sulfur species. They are expected to react with each other. For example, sulfur species may react with NO , CO etc., in the gas phase. Potassium species may react with coal-bound chlorine. A potassium-sulfur reaction model in an MHD system is completed only after all the possible reactions are considered and included.

LIST OF REFERENCES

LIST OF REFERENCES

1. J.H. Lanier, R.C. Attig and P.R. Kulesza, "Sulfur Dioxide and Nitrogen Oxide Emissions Control in a Coal-Fired MHD System", 1979 ASME Winter Annual Meeting, New York, NY, December 2-10, 1979.
2. T.R. Johnson, P.E. Blackburn, C.E. Johnson, and L.S. Chow, "Seed-Slag Chemistry – Implication for MHD Plant Design", Prepared for Presentation at the Seventh International Conference on MHD Electrical Power Generation, Cambridge, Massachusetts, June 16-20, 1980.
3. S. Gordon and B.J. McBride, "Computer Program for Calculation of Complex Chemical Equilibrium Compositions, Rocket Performances, Incident and Reflected Shocks, and Chapman-Jouguet Detonations", NASA Lewis Research Center, NASA SP-273, 1971.
4. R.M. Kendall and J.T. Kelly, "Premixed One-Dimensional Flame (PROF) Code User's Manual", EPA-600/7-78-172a, August, 1978.
5. J. Woodring, "Documentation of the UTSI COAL Computer Code", Internal Report, OR-10815-15, UTSI, Tullahoma, TN, 1980.
6. C.A. Luongo and C.H. Kruger, "Modeling of Slag/Seed Interaction Phenomena in Coal-Fired MHD Generators", 22nd Symposium on Engineering Aspects of Magnetohydrodynamics (SEAM 22), Mississippi State University, Starkville, Mississippi, June 26-28, 1984.
7. JANAF Thermochemical Tables, J. Phys. Chem. Ref. Data, Vol. 14, Suppl. 1, pp 1418-1422, 1985.

8. L.G. Piper, G. Wilemski, and P.F. Lewis, "Thermodynamic Properties of Gas-Phase Potassium Sulfide Species", *High Temperature Science* 14, 1-9(1981).
9. Private Communication with L.W. Crawford, Professor of Chemical Engineering, The University of Tennessee Space Institute, Tullahoma, TN, 1990
10. D.R. Knisley, "Reaction Kinetics of the Downstream MHD Process Gas Before Secondary Combustion". M.S. Thesis, The University of Tennessee, Knoxville, TN, 12, 85.
11. Private Communication with L.W. Crawford, Professor of Chemical Engineering, The University of Tennessee Space Institute, Tullahoma, TN, 1990
12. L.D. Smoot and D.T. Pratt, "Pulverized-Coal Combustion and Gasifications, Theory and Applications for Continuous Flow Processes", Plenum Press, p197, 1979.
13. W.M. Swift, A.F. Panek, G.W. Smith, G.F. Vogel and A.A. Jonke, "Decomposition of Calcium Sulfate: A Review of the Literature", Report ANL-76-122, Argonne National Laboratory, US ERDA, Argonne, IL(1976).
14. W.H. Wiser, "Conversion of Coal to Liquids—Research Opportunities, in Research in Coal Technology: University's Role", pp. 73-94, Report CONF-741091, US ERDA, Washington, D.C.(1975).
15. G.L. Tingey and J.R. Morrey, "Coal Structure and Reactivity", Battelle Energy Program Report, Battelle Northwest Laboratories, Richland, Washington, D.C.(1975).

16. P.R. Solomon, "The Evolution of Pollutants during the Rapid Devolatilization of Coal", Report R76-952588-2, United Technologies Research Center, East Hartford, Conn.(1977).
17. A. Attar, A.H. Corcoran, and G.S. Gibson, "Transformation of Sulfur Functional Groups during Pyrolysis of Coal", in Proceedings of 172nd National Meeting of the American Chemical Society, Division of Fuel Chemistry, Vol. 21, pp. 106-111, American Chemical Society, Washington, D.C.(1976).
18. C.F. Cullis and M.F.R. Mulcahy, "The Kinetics of Combustion of Gaseous Sulfur Compounds", Combustion and Flame 18, 225-292(1972).
19. S. Srinivasachar, J.J. Helble, D.O. Ham and G.Domazetis, " A Kinetic Description of Vapor Phase Alkali Transformations in Combustion Systems", Prog, Energy Combust. Sci., Vol 16, pp. 303-309, 1990.
20. M. Steinberg and K. Schofield, "The Chemistry of Sodium with Sulfur in Flames", Prog, Energy Combust. Sci., Vol 16, pp. 311-317, 1990.
21. Jandel Scientific, "SigmaPlotTM", Scientific Graphing Software, Version 4.0, December, 1989.

APPENDICES

APPENDIX A

CALCULATION OF POTASSIUM LOSS AS K_2O IN THE RADIANT FURNACE SLAG

Major part of potassium is lost in the radiant furnace slag. Given below is an example that calculates the potassium loss as K_2O in the slag.

For test LMF4-R, the seed K_2CO_3 is 11.3225 lb/100 lb coal, if $K_2/S=1.0$. This value is calculated from M-COAL code. Of this seed,

$$K_2O = 11.3225 \times 0.68158 = 7.7172 \text{ lb/100 lb coal}$$

$$CO_2 = 11.3225 \times 0.31842 = 3.6053 \text{ lb/100 lb coal}$$

From the coal analysis data, coal ash = 9.32% of the coal(normalized)

From the coal ash analysis, K_2O = 5.07% of the ash(normalized)

From the slag analysis data, K_2O = 17.44% of the slag(normalized).

We have assumed that 70 %(wt) of the coal ash is rejected at Radiant Furnace as slag. Thus, K_2O remaining in the system after slag removal can be obtained as

$$K_2O = 7.7172 - 9.3225 \times 0.70 \times (17.44 - 5.07)/100 \\ = 6.9100 \text{ lb/100 lb coal.}$$

Potassium lost to the slag as K_2O can thus be calculated as

$$K_2O\% = \frac{7.7172 - 6.9100}{7.7172} = 10.5\%(lost)$$

In the equilibrium calculations, potassium lost as K_2O in the slag was assumed to be 10 %(wt) of the K_2O contained in the seed.

Finally, the inputs to the NASA code of the seed are

$$CO_2(g) = 3.6053 \text{ lb/100 lb coal}$$

$$\text{K}_2\text{O(s)} = 6.9100 \text{ lb/100 lb coal}$$

It should be noted that the other part of potassium loss – potassium tied up with the rest of the coal ash (about 30% (wt)) was not taken into account in the equilibrium calculations.

APPENDIX B

H₂S MEASUREMENTS IN THE CFFF FOR EARLY TESTS

THE UNIVERSITY OF TENNESSEE SPACE INSTITUTE

MEMORANDUM

Date: January 17, 1985
To: J. W. Muehlhauser
From: W. E. Baucum *WEB*
Subject: Correction of LMF3 H₂S Measurements

It was recently discovered that the calibration gas used to calibrate H₂S gas measurements during the LMF3 test series has partially decomposed. This has caused the measurements to yield higher values that are incorrect. A new H₂S calibration gas has been purchased and the previous measurements have been recalibrated using this new standard. The following table gives the corrected H₂S concentration values:

<u>Test</u>	<u>Time</u>	<u>Sample Point</u>	<u>H₂S Concentration (ppm)</u>
LMF3A-3	12:49	SCI	1800
LMF3B-1	12:15	RF1	140
LMF3B-1	12:20	SCI	300
LMF3B-2A	8:45	SCI	1640
LMF3B-2B	8:07	SCI	2170
LMF3B-2B	9:47	SCI	2230
LMF3B-2B	11:39	SCI	2480

Please correct your previous records of test data to show these new values.

WEB/bh

xc: R.C. Attig
L. Crawford
J. Foote
D. Jackson
D. Knisley
P. Lynch
T. Shaver

During LMF3B-1, ~~an~~ H₂S measurements were made at SCO and ~~the~~ no H₂S was detected (estimate detection limit ≤ 10 ppm)

APPENDIX C

THE INPUT FILE FOR PROF MODELING

The following input file was used to model the chemical kinetics in the sampling probe at RF1 location for LMF4-U test:

```

stoi 85 2300 4U-RF1
37 0 37 32 1 0 1 1 4 0 1 0 0 0 0 0
561. 0. 1. 2300. 0. 2500.
1. 1. 1. 1. 1. 1. 1. 1.
1. 1. 1. 1. 1. 1. 1. 1.
1. 1. 1. 1. 1. 1. 1. 1.
1. 1. 1. 1. 1. 1. 1. 1.
05.08E-01 05.08E-01 05.08E-01 05.08E-01 05.08E-01 05.08E-01 05.08E-01 05.08E-01
05.08E-01 05.08E-01 05.08E-01 05.08E-01 05.08E-01 05.08E-01 05.08E-01 05.08E-01
05.08E-01 05.08E-01 05.08E-01 05.08E-01 05.08E-01 05.08E-01 05.08E-01 05.08E-01
1
1 0.08
1 335.
CO 1.1443-1 .1-3 .9830
CO2 1.8763-1 .1-2 .8
H 1.3100-3 .1-3 5.1557
H2 1.8610-2 .1-3 3.5333
H2O 1.6822-1 .1-2 1.2980
NO 5.4000-4 .001 1.3700
N2 4.9809-1 .41529 .9732
O 9.0000-4 .1-3 1.4158
HO 1.8900-3 .1-3 1.3475
O2 3.5000-4 .1-2 1.0468
CN 1.365-11 1.-7 .98
CHN 1.8322-9 1.-7 .98
HNO 4.8050-8 1.-7 .95
HO2 9.653 -8 .1-3 .9016
N 5.865 -8 1.-7 1.4300
NCO 1.004-10 1.-7 .90
HN 4.438 -9 1.-7 1.2
H2N 1.624 -8 1.-7 1.2
H3N 1.3223-8 1.-7 1.15
NO2 5.776 -8 .1-6 .8
N2O 3.949 -8 1.-7 .85
CHO 3.305 -8 .24-9 .9604
K 2.6400-3 .1-3 .9
HKO 2.5100-3 .1-3 .9
KO 1.0000-5 .1-3 .9
O2S 2.2300-3 5.-3 .2
S 7.8830-6 1.-7 1.
HS 4.1059-6 1.-7 1.
S2 9.9919-8 1.-7 1.
H2S 1.0952-6 1.-7 1.
OS 1.9000-4 1.-7 1.
O3S 2.760 -7 1.-7 1.
NS 4.6660-8 1.-7 1.
COS 3.9541-7 1.-7 1.
CS 1.104-10 1.-10 1.
CS2 1.824-13 1.-13 1.
OS2 1.6713-8 1.-8 .7
END
112
CO2 M CO O .38000E+31-4. 134.021
CO HO CO2 H .15000E+081.3 -.765
CO O2 CO2 O .32000E+130. 50.
H2 M H H .21000E+16.07 103.83
HO O M HO2 .16000E+21-1.5 0.
H O2 M HO2 .30000E+160. -1.
H2O M HO H .23000E+25-2. 122.6
H HO H2 O .27000E+18-.94 14.69
H HO2 HO HO .25000E+150. 1.9
HO H2 H H2O .25000E+140. 5.2
HO HO H2O O .60000E+130. 1.
HO O H O2 .63000E+12.5 0.
HO2 H O2 H2 .25000E+140. .7
HO2 O HO O2 .50000E+140. 1.

```

CHN	HO	CN	H2O	.20000E+12.6		5.
CN	CO2	NCO	CO	.37000E+130.		0.
CN	HO	NCO	H	.62000E+140.		0.
CN	H2	CHN	H	.62000E+130.		5.3
CN	O	CO	N	.63000E+12.5		0.
NCO	H	HN	CO	.50000E+12.5		6.87
CO	HNO	CO2	HN	.10000E+12.5		21.0
H	NO	M	HNO	.20000E+170.		0.
NO	O	M	NO2	.14000E+22-1.82		0.
N2O		M	N2	O	.40000E+150.	51.4
H	HNO		H2	NO	.10000E+140.	2.5
H	N2O		HO	N2	.80000E+140.	15.
HN	NO		H	N2O	.90000E+10.75	00.
H	NO2		HO	NO	.32000E+150.	1.5
HNO	HO		H2O	NO	.36000E+140.	0.
HNO	O		HO	NO	.50000E+12.5	0.
HNO	O		HN	O2	.10000E+12.5	7.
HO	N2O		HO2	N2	.32000E+140.	15.
N2	O		NO	N	1.84+14	0.0 76.25
O	NO		N	O2	2.36+09	1.0 38.65
NO	H		N	HO	2.22+14	0.0 50.5
HN	H		N	H2	.63000E+12.5	8.
HN	HO		H2O	N	.50000E+12.5	2.
HN	HO		NO	H2	.50000E+12.5	2.
HN	O		NO	H	.63000E+12.5	0.
H2N	H		HN	H2	.14000E+12.67	4.3
H2N	HO		HN	H2O	.30000E+11.68	1.3
H2N	O		HN	HO	.92000E+12.5	0.
H2N	H2N		H3N	HN	.17000E+12.63	3.6
H3N	HO		H2N	H2O	.17600E+13.00	1.7
H3N	H		H2N	H2	.24600E+14.00	17.07
H2N	NO		N2	H2O	.50000E+130.	0.
H3N	O		H2N	HO	.15000E+130.	6.
H3N	O2		H2N	HO2	.50000E+12.5	56.
NO	HO2		NO2	HO	.50000E+12.5	3.52
HN	HO		HNO	H	5.00+11	.5 5.62
CO	N2O		CO2	N2	3.00+11	17.2
CHO		M	H	CO	1.55E+14	0. 14.7
CHO	H		CO	H2	2.00E+14	0. 0.
CHO	O		CO	HO	5.50E+12	0.5 0.
CHO	O		CO2	H	5.50E+12	0.5 0.
CHO	HO		CO	H2O	3.00E+12	1.0 0.
CHO	O2		CO	HO2	5.00E+11	0.5 0.83
H2N	O		H	HNO	2.10E+12	0.0 0.00
CO2	N		NO	CO	2.00E+11	-5 8.00
NO	NO		N2O	O	1.29E+12	0.0 63.8
HNO	HNO		N2O	H2O	.300E+12	0.0 3.5
NO	HNO		N2O	HO	2.00E+12	0.0 26.
NO	NO		N2	O2	3.10E+13	0.0 63.1
K	H2O		HKO	H	6.02+13	0. 39.7
K	HO	M	HKO		2.18+20	-1. 0.
KO	HO		HKO	O	2.00+11	0.5 8.
KO	H		HO	K	2.00+11	0.5 8.
HS	S		H	S2	6.31+11	.5 .000
HS	H		S	H2	6.31+11	.5 0.000
H2S	H		HS	H2	9.03+12	.0 1.700
HS	HS		H2S	S	1.00+14	.0 1.420
HO	H2S		H2O	HS	1.40+13	.0 .894
OS	HO		H	O2S	6.46+14	.0 2.10
S	HO		OS	H	6.31+11	.5 .000
HS	O		OS	H	6.31+11	.5 .000
O	H2S		HS	HO	4.40+12	.0 3.298
HS	O		S	HO	6.31+11	.5 8.00
OS	O2		O2S	O	1.81+11	.0 5.600
S	O2		OS	O	6.31+11	.5 0.
O	S2		OS	S	6.31+11	.5 .0

APR '86

DOE/ET/11313-

J&J

KRUG 17SYMP 1
 KRUG 17 SYMP
 ROOSE 11 SH'

(5.146)
 D-LP225
 (5.20)
 (5.24)
 (5.25)
 (5.26)
 (5.27)
 (5.28)
 LEVY
 EXXON
 CRCP176
 15 C SY P83.
 CRC P176
 CRC P176

31M
 32M
 33M
 34M
 35M
 18M
 36M
 37M
 38M
 39M
 16M
 22M
 30M

OS	OS		O2S	S	4.10+11	.0	3.23	40M
S	H2O		HS	HO	4.40+12	.0	28.	41M
S	S	M	S2		1.00+18	-1.	0.	42M
S	O	M	OS		5.50+13	.0	1.788	43M
S	H	M	HS		7.20+15	.0	0.	44M
H2S		M	HS	H	2.00+14	.0	74.	45M
OS	O	M	O2S		1.22+22	-1.84	0.	46M
O2S	O	M	O3S		4.00+20	-4.	5.3	WMERL1
O3S	O		O2S	O2	2.80+14	0.	12.0	WMERL3A
N	OS		NO	S	6.31+11	.5	2.	WENCF83
NO	S		NS	O	1.00+12	.5	34.8	WENCF83
NS	O		OS	N	6.31+11	.5	8.	WENCF83
N	NS		N2	S	6.31+11	.5	0.	WENCF83
N	HS		NS	H	6.31+11	.5	8.	WENCF83
OS	HNO		O2S	HN	6.31+11	.5	8.	LWC MAR 18 1
NO	NS		N2O	S	6.31+11	.5	8.	LWC MAR 18 1
N	O2S		NO	OS	2.00+11	.5	8.0	LWC MAR 19 1
H2N	HS		H2S	HN	6.31+11	.5	0.0	LWC JUN 13 1
CS2	O		CS	OS	.50000E+140.		1.9	HARDY&GARJ
CS2	O		COS	S	.17000E+130.		1.2	
CS2	O		CO	S2	.32000E+130.		1.0	
COS	O		CO	OS	.60000E+140.		5.5	
COS	O		CO2	S	.12000E+150.		11.	
CS	O		CO	S	.11000E+140.		41.	
CS2	S		CS	S2	.15000E+140.		00.	
COS	S		CO	S2	.90000E+120.		2.5	
COS	OS		CO2	S2	.10000E+090.		0.	
CS	O2		CO	OS	.55000E+080.		2.	
CS	O2		COS	O	.31000E+100.		9.5	
CS	OS		CO	S2	.10000E+140.		00.	
CS	S	M	CS2		.51000E+25-3.		00.	
CO	S	M	COS		.29000E+26-3.6		00.	

VITA

Jun Li was born on December 25, 1962 in Hangzhou, Zhejiang Province, China. He graduated from the Second High School at Anji County in 1979. The following fall he entered Zhejiang University and received a Bachelor's degree in Chemical Engineering in July, 1983. He then worked in the Beijing Chemical Industrial Research and Development Institute as a research engineer for about a year. In June, 1984, he became a patent examiner in the Patent Office of China, and worked there until December, 1988.

He came to America and joined the University of Tennessee Space Institute in January, 1989. In May, 1991, he graduated from UTSI with a Master of Science degree in Chemical Engineering.